THE NUMERICAL CALCULATION OF THE FLOW FIELD AROUND A REENTRY BODY

GASL Report TR-231

by

E. Kennedy and A. Fields

April 24, 1961

Reissued September 18, 1962

The work reported in this document was performed at General Applied Science Laboratory, Inc. for M. I. T. Lincoln Laboratory under Subcontract No. 226; this work was supported by the U.S. Advanced Research Projects Agency under Air Force Contract AF 19(604)-7400.

Publication of this technical documentary report does not constitute Air Force approval of the report's findings or conclusions. It is published only for the exchange and stimulation of ideas.

THE NUMERICAL CALCULATION OF THE FLOW FIELD AROUND A REENTRY BODY

TECHNICAL REPORT NO. 231

By E. Kennedy and A. Fields

SUBCONTRACT NO. 226

Prepared For

Massachusetts Institute of Technology
Lincoln Laboratory
Lexington 73, Massachusetts

Prepared By

General Applied Science Laboratories, Inc.
Merrick and Stewart Avenues
Westbury, L.I., New York

April 24, 1961

Approved By _____
Antonio Ferri
Technical Director

TABLE OF CONTENTS

Section	Title	Page
I	Introduction	1
II	Method of Calculation	2
III	Results	4
IV	Conclusions	5
	References	6
	Figures 1 - 3, 4a - ℓ, 5a - ℓ, 6a - ℓ.	7
Addendum	Table I and Revised Figs. 1, 2 and 3.	46

THE NUMERICAL CALCULATION OF THE FLOW FIELD AROUND A REENTRY BODY

By E. Kennedy and A. Fields

I INTRODUCTION

The flow field around the Trailblazer I body (a sphere with a short cylindrical afterbody) has been calculated for three flight conditions - 18,900 feet per second at 150,000 feet, 20,200 ft. per second at 200,000 feet, and 20,400 feet per second at 250,000 feet.

In the study of flow fields about blunt bodies at these speeds and altitudes, not only must the classical assumption of a calorically perfect gas be abandoned but account must be taken of various chemical reactions which become significant at these conditions. Each reaction introduces a characteristic time which, if comparable with the time of travel through the region of interest, will cause deviations from thermodynamic equilibrium and consequently some elaborate description of the thermodynamic behavior of the fluid is required. In the case of the relatively high altitudes (above 150,000 feet) and the speeds of current interest it has been established (Reference 3) that insofar as the gross thermodynamic properties (i.e., pressure, temperature, etc.) are concerned, it is sufficient to consider only the five components N_2, N, O_2, O and NO and further that the equilibrium concentrations of these are reached relatively close to the bow shock and thereafter remain fixed. This assumption governs the calculations reported herein.

II METHOD OF CALCULATION

The method of calculation used at GASL for blunt nosed bodies of revolution has been outlined by Vaglio-Laurin (Ref. 1) and Vaglio-Laurin and Ferri (Ref. 2). In short, the procedure is to guess a shock shape in the nose region and then to develop the flow field in the slightly supersonic region by the characteristics method. These data serve as input data for a calculation of the purely subsonic region. The result of this second calculation is a body shape which may be compared with the true shape and, if necessary, the assumed shock shape changed. In fact, it has developed that for most round nosed bodies a single guess will suffice. The calculation in the purely supersonic region then proceeds to generate the flow field and shock shape downstream of the nose. These calculations have been programmed for the IBM 704. There is no way in these programs to generate a shock in a nonuniform flow and so the calculation must stop at corners or surfaces causing shocks within the rotational region downstream of the bow shock. In the case of the flow field around the Trailblazer I body, there are two such shocks, one on the body at roughly 2 1/4 nose radii from the nose and the second at the closing of the wake. If it is desired to continue the calculation beyond such a point, the shock shape must be estimated and conditions downstream of it used as input data for the continuation of the original program. (These programs are being extended to automatically generate such secondary shocks and thus avoid the laborious procedure presently being used).

The general procedure outlined above is independent of the thermodynamic behavior of the gas about which some a priori assumption must be made. This assumption amounts to deciding which of the myriad possible reactions are significant. It was originally decided to treat nonequilibrium effects as perturbations on a basic flow which would be either one in thermodynamic equilibrium or one of constant chemical composition along streamlines. This basic flow field could be done independently and then the linearized equations obtained by neglecting squares of the perturbations solved to get first order departures from the basic field. This proposed method was abandoned after it was shown in Reference 3 that for the cases of interest, the mass fractions of the

major constituents did not vary (along streamlines) from their initial values behind the bow shock. Furthermore the flow in the subsonic or slightly supersonic region was shown to be in thermodynamic equilibrium which made available for use an existing program. The degree of ionization on the other hand could be calculated from the reaction $N+O \rightarrow NO^{+}+e^{-}$, this to be taken in equilibrium at the temperature and density determined by the frozen flow field. As mentioned above, the justification for these simplifications results from a detailed calculation of the rate processes in Reference 3 and no further discussion will be given here.

With these assumptions, the basic characteristics equations were programmed for the IBM 704*. The detailed procedure used was then to assign a shock shape and generate (with the assumption of thermodynamic equilibrium) the flow in the transonic region. These data then served as input to the frozen flow calculation which kept the composition constant along streamlines. Since additional streamlines entered the calculation as the bow shock was developed, it was necessary to calculate the chemical composition at each new point on the shock. The significant reactions were taken to be $N_2 \rightleftharpoons 2N$, $O_2 \rightleftharpoons 2O$ and $N+O \rightleftharpoons NO$ and accordingly, at each point on the shock the equilibrium concentrations of these five were computed.

---

* (Very capably by Mr. Edward Lieberman of GASL)

III RESULTS

The shock and streamline shapes are shown in Figs. 1, 2 and 3 for 150, 200 and 250,000 feet respectively. A cylinder (with radius 1/2 that of the nose) has been assumed to extend downstream from the wake shock. This addition is suggested by photographs of actual wakes where the wake shocks begin at roughly this distance from the axis and furthermore and possibly more to the point the characteristics equations require special treatment if they are to be used near the axis.

The streamlines sketched in these figures show that the air entering the steep portion of the bow shock extends over a large portion of the shock layer downstream of the body. This has been noted earlier (Ref. 4) for the case of thermodynamic equilibrium. Not unexpectedly then the density profiles in the wake show a relatively constant density over the inner portion and a rapid rise in the outer portion.

The distributions across the shock layer of temperature, density, pressure and electron concentration are given in Figs. 4, 5 and 6 for various streamwise stations. At stations on the body these exhibit the rather unusual characteristic that the temperature is lowest on the body. This is a result of the assumed constant composition which does not allow the energy of dissociation to be released as the flow expands around the body. The increasing temperature and decreasing concentration of atomic species in the direction normal to the axis causes the electron concentration profiles to have maxima at these stations.

At stations in the near wake, the profiles exhibit discontinuities corresponding to the trailing and wake shocks. (It should be pointed out that these shocks have been estimated both in position and strength and are the more in error the further from the body). It is seen that these shocks cause order of magnitude increases in electron concentration and therefore cannot be neglected.

In the far wake the discontinuities due to these shocks has disappeared and the various parameters vary monotonically from body to shock.

IV CONCLUSIONS

The flow field around a typical reentry body has been calculated with the assumption of frozen chemical composition along streamlines. The effect of additional shocks in the flow field has been calculated and leads to order of magnitude changes in electron density in the wake. It is thus apparent that some effort should be made to improve the accuracy of this part of the calculation.

REFERENCES

1. Vaglio-Laurin, R., On the Determination of Real Gas Flows About Blunt-Nosed Bodies, General Applied Science Laboratories, Inc., Technical Report No. 104, July 1959.

2. Vaglio-Laurin, R. and Ferri, Antonio, Theoretical Investigation of the Flow Field About Blunt-Nosed Bodies in Supersonic Flight, Journal of the Aero/Space Sciences, Vol. 25, No. 12, December 1958.

3. Bloom, M.H. and Steiger, M.H., Inviscid Flow with Nonequilibrium Molecular Dissociation for Pressure Distributions Encountered in Hypersonic Flight, Journal of the Aero/Space Sciences, Vol. 27, No. 11, November 1960.

4. Feldman, S., Numerical Comparison Between Exact and Approximate Theories of Hypersonic Inviscid Flow Past Slender Blunt-Nosed Bodies, A.R.S. Journal, Vol. 30, No. 5, May 1960.

FLOW FIELD DETAILS

150,000 FT.

V_∞ = 18,900 FT./SEC.

FIG. 1

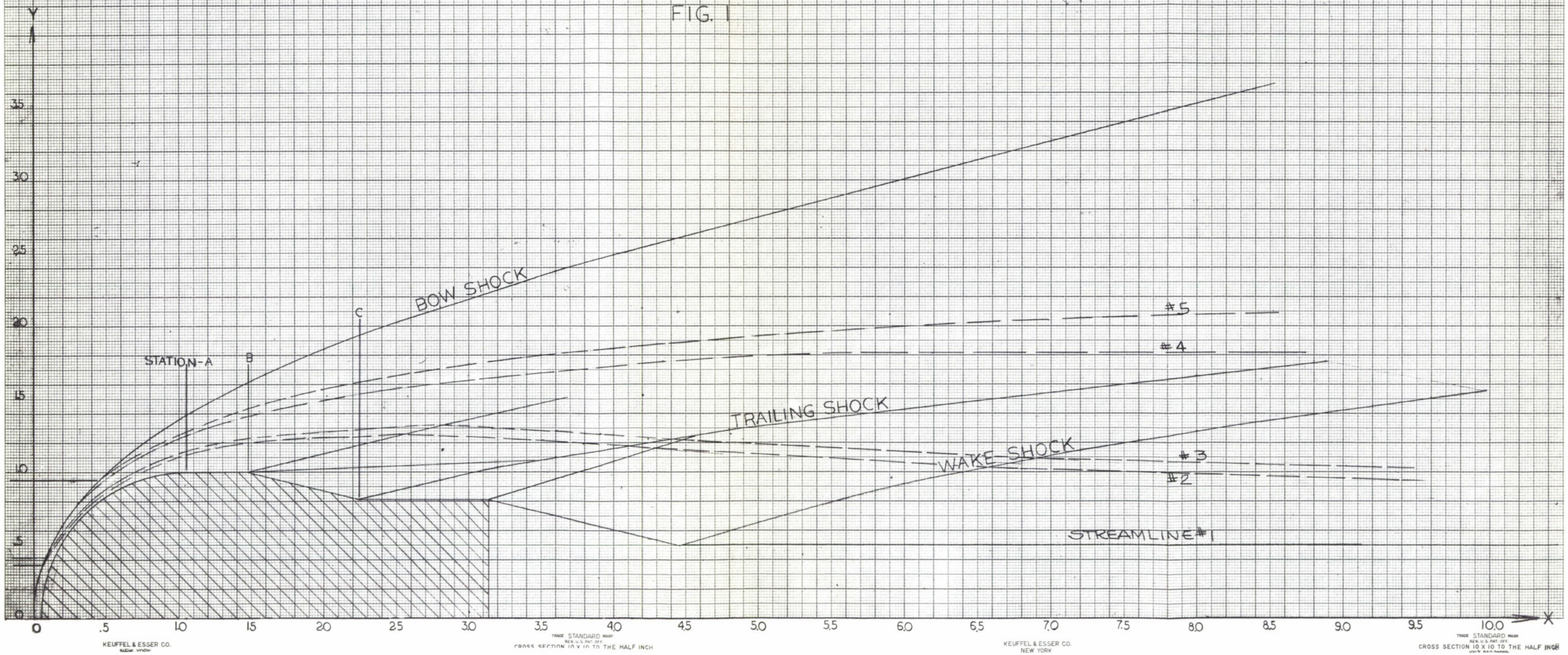

KEUFFEL & ESSER CO.
MADE IN U.S.A.

TRADE STANDARD MARK
REG. U.S. PAT. OFF.
CROSS SECTION 10 X 10 TO THE HALF INCH

KEUFFEL & ESSER CO.
NEW YORK

TRADE STANDARD MARK
REG. U.S. PAT. OFF.
CROSS SECTION 10 X 10 TO THE HALF INCH

FLOW FIELD DETAILS
200,000 FEET
V_∞ = 20,200 FT./SEC.

FIG. 2

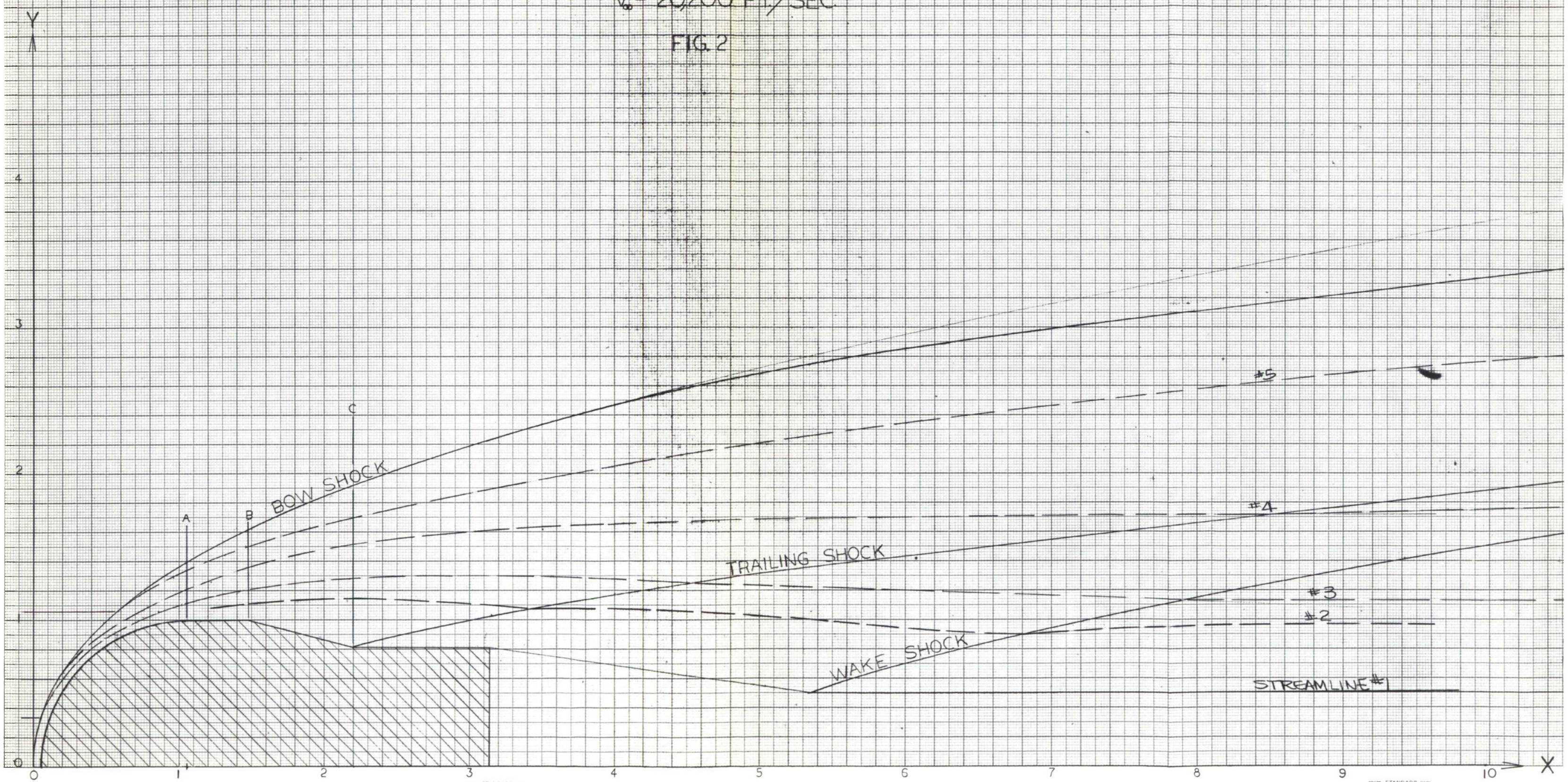

KEUFFEL & ESSER CO.
NEW YORK

TRADE STANDARD MARK
REG. U.S. PAT. OFF.
CROSS SECTION 10 X 10 TO THE HALF INCH
100% RAG PAPER
MADE IN U.S.A.

FLOW FIELD DETAILS

250,000 FEET

V_∞ = 20,400 FT./SEC.

FIG. 3

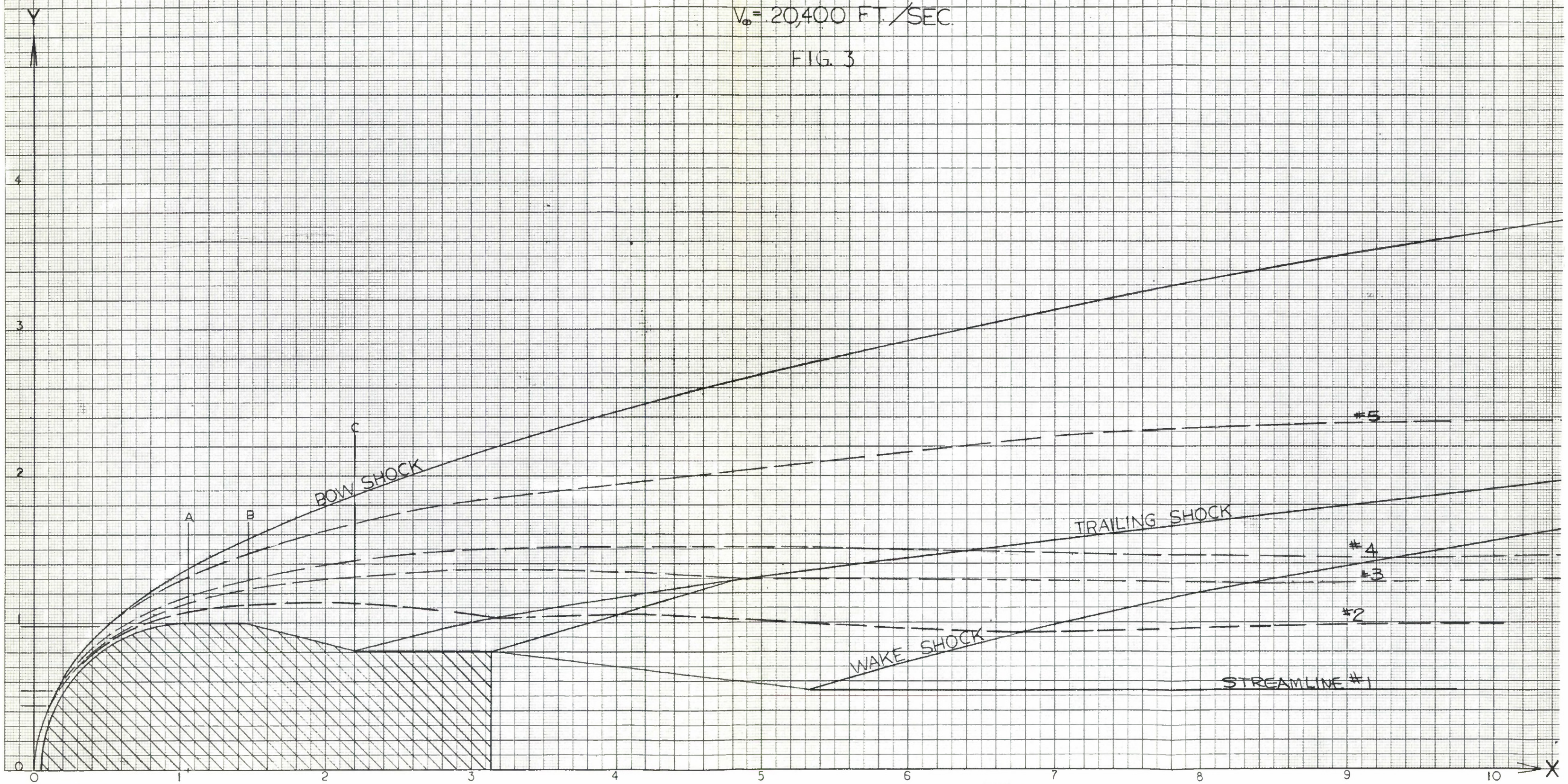

Figure 4a.

PRESSURE RATIO ACROSS SHOCK LAYER

150,000 feet

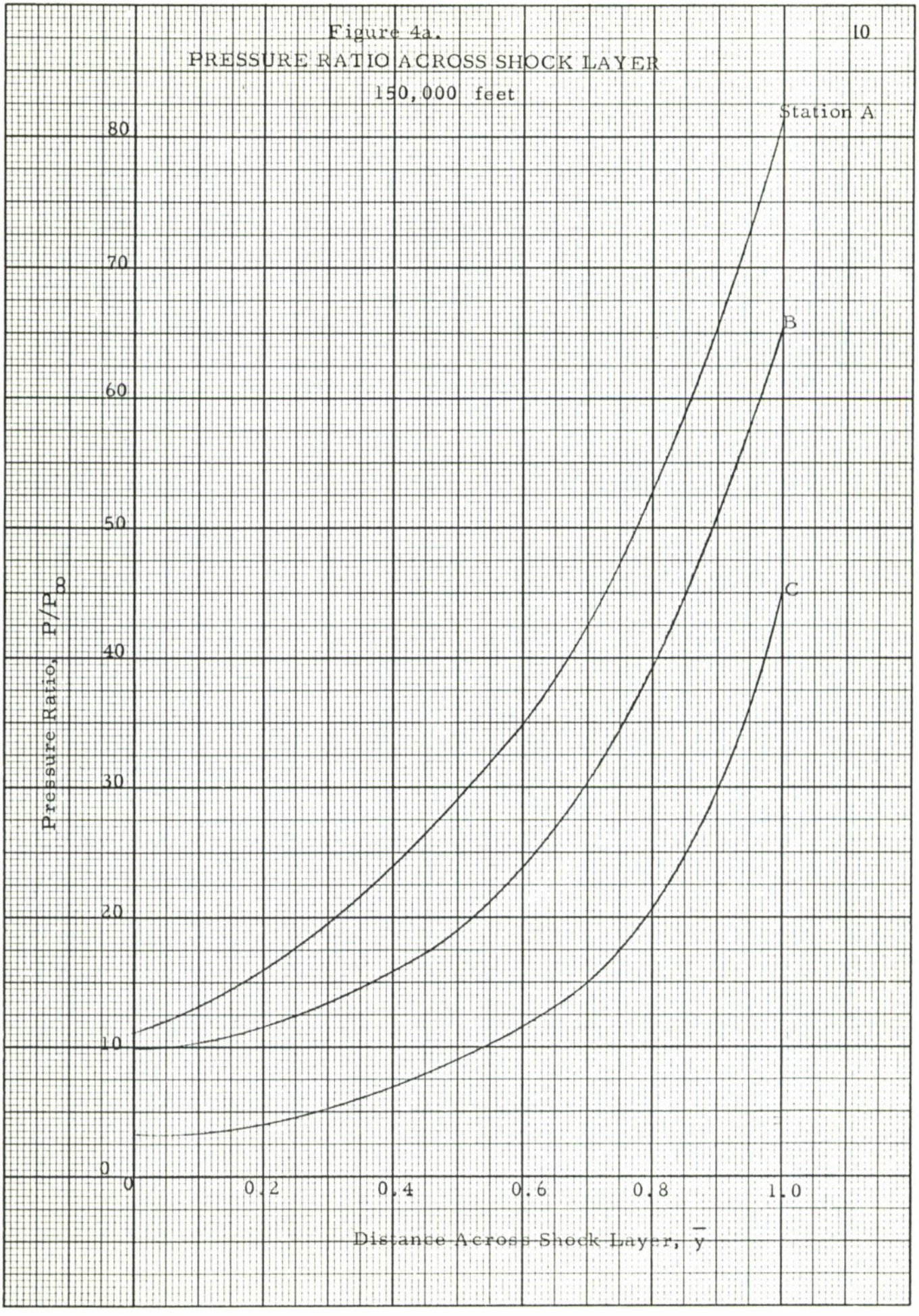

Figure 4b.
DENSITY RATIO ACROSS SHOCK LAYER
150,000 feet

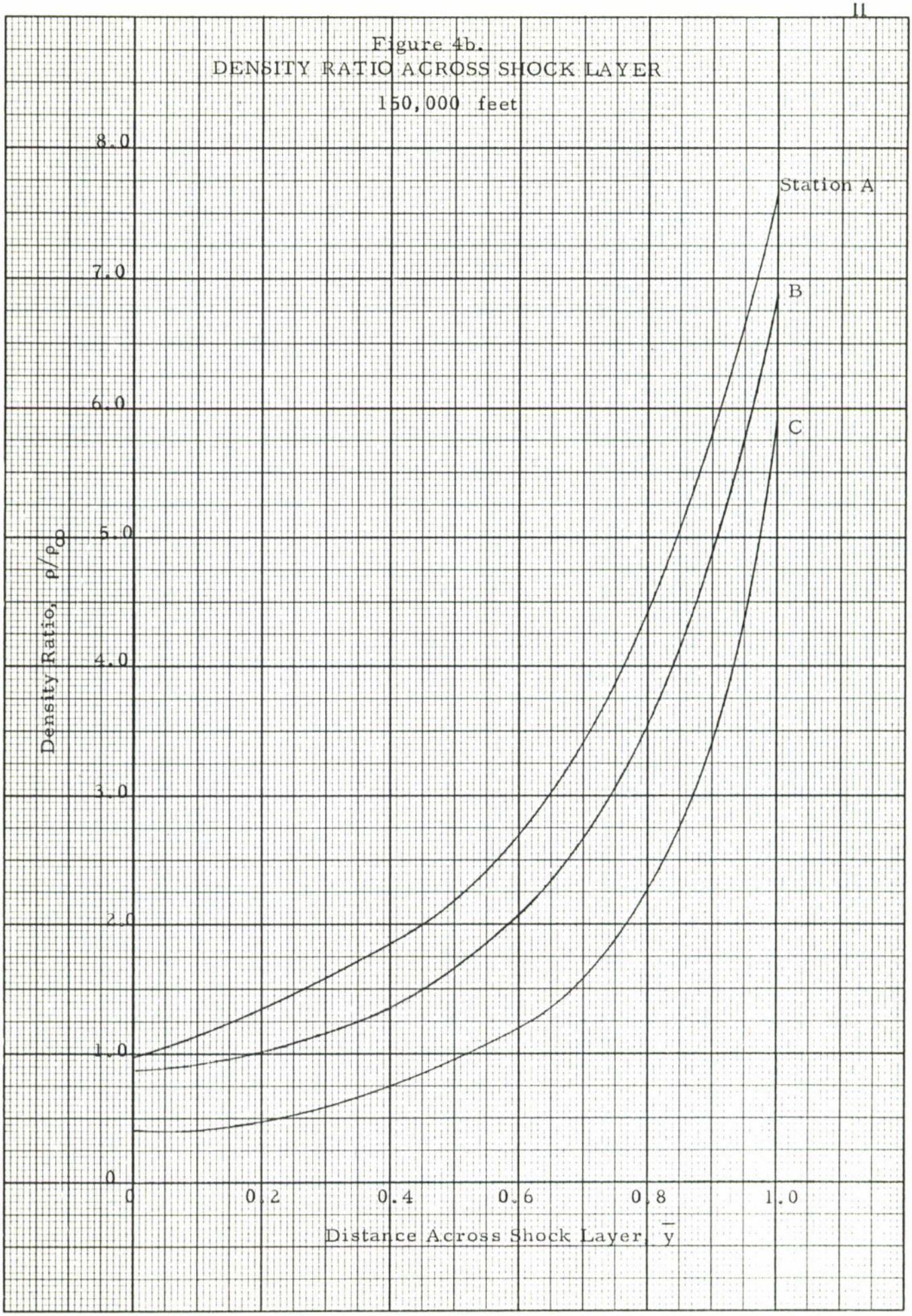

Figure 4c.

TEMPERATURE DISTRIBUTION ACROSS SHOCK LAYER

150,000 feet

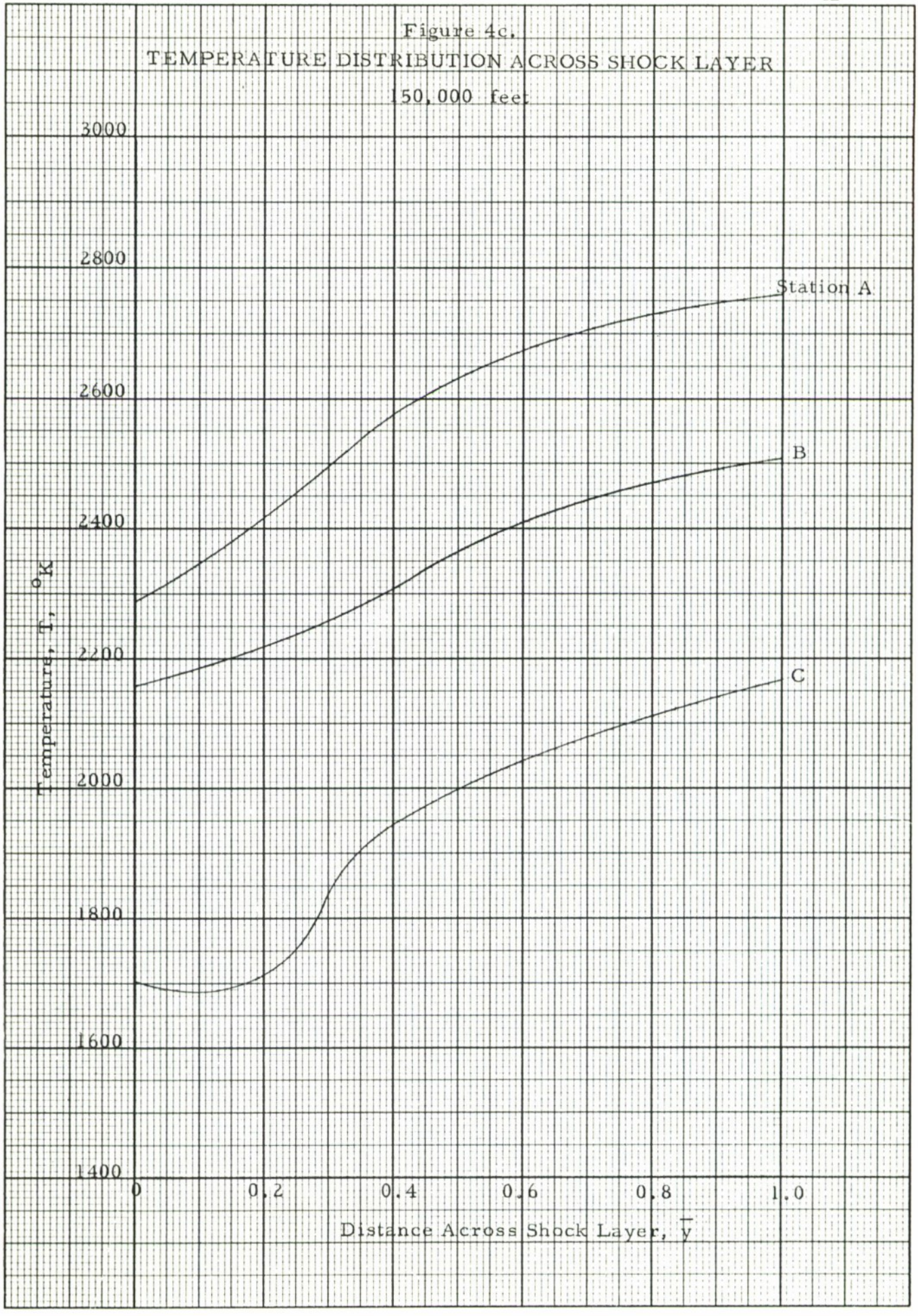

Figure 4d.
ELECTRON DENSITY DISTRIBUTION ACROSS SHOCK LAYER

150,000 Feet

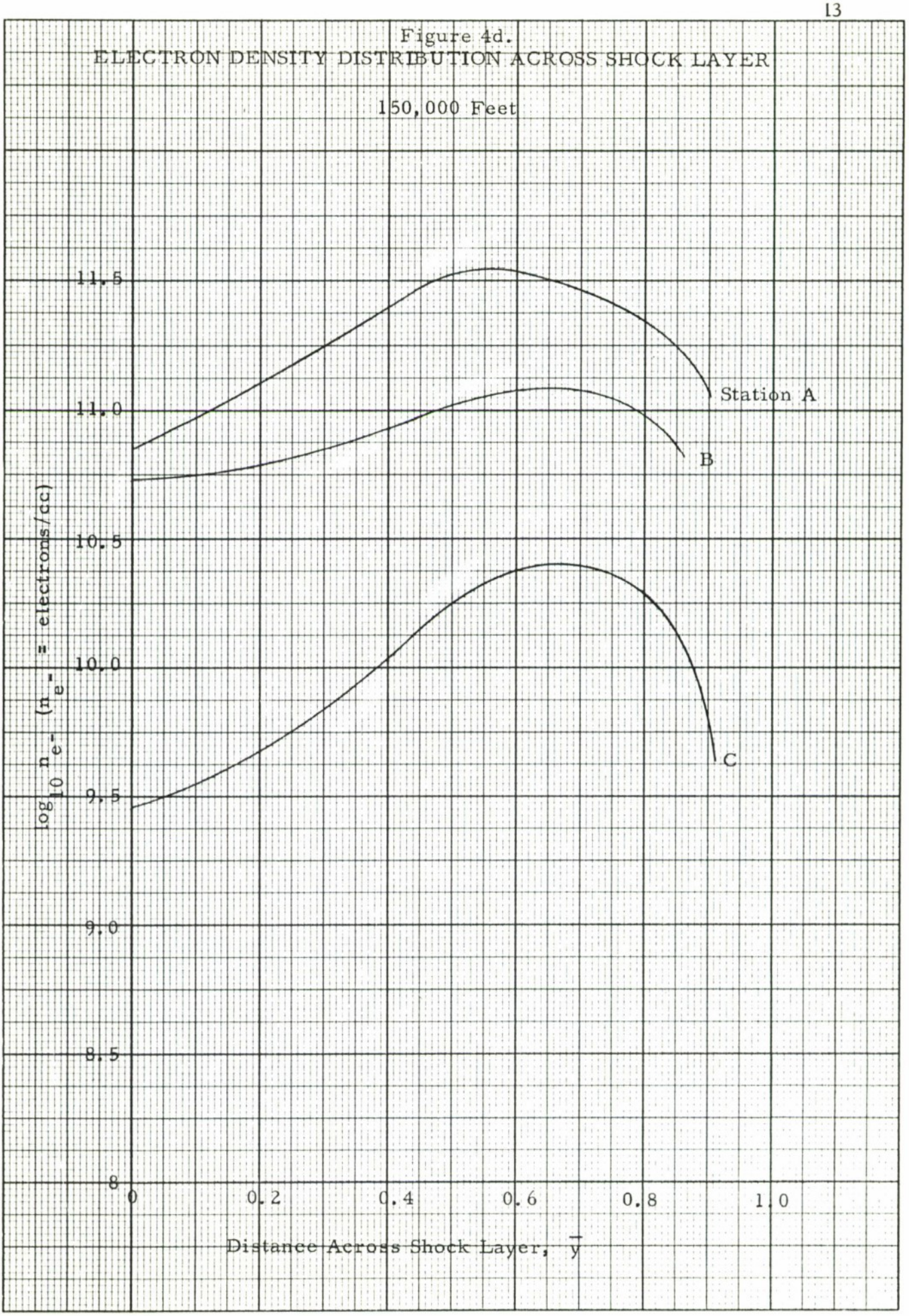

Figure 4e.
Pressure Ratio Across Shock Layer

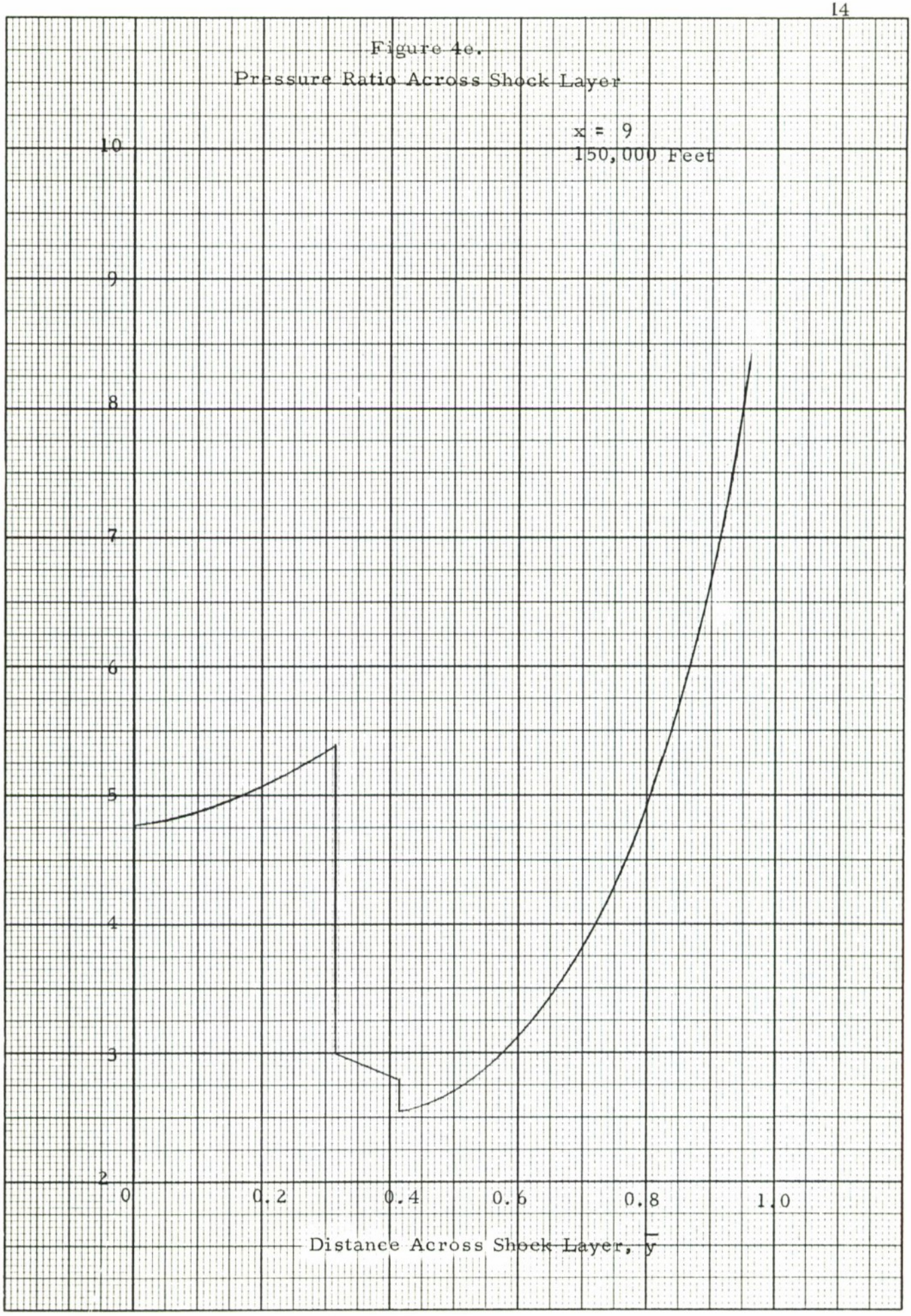

Figure 4f.
DENSITY RATIO ACROSS SHOCK LAYER

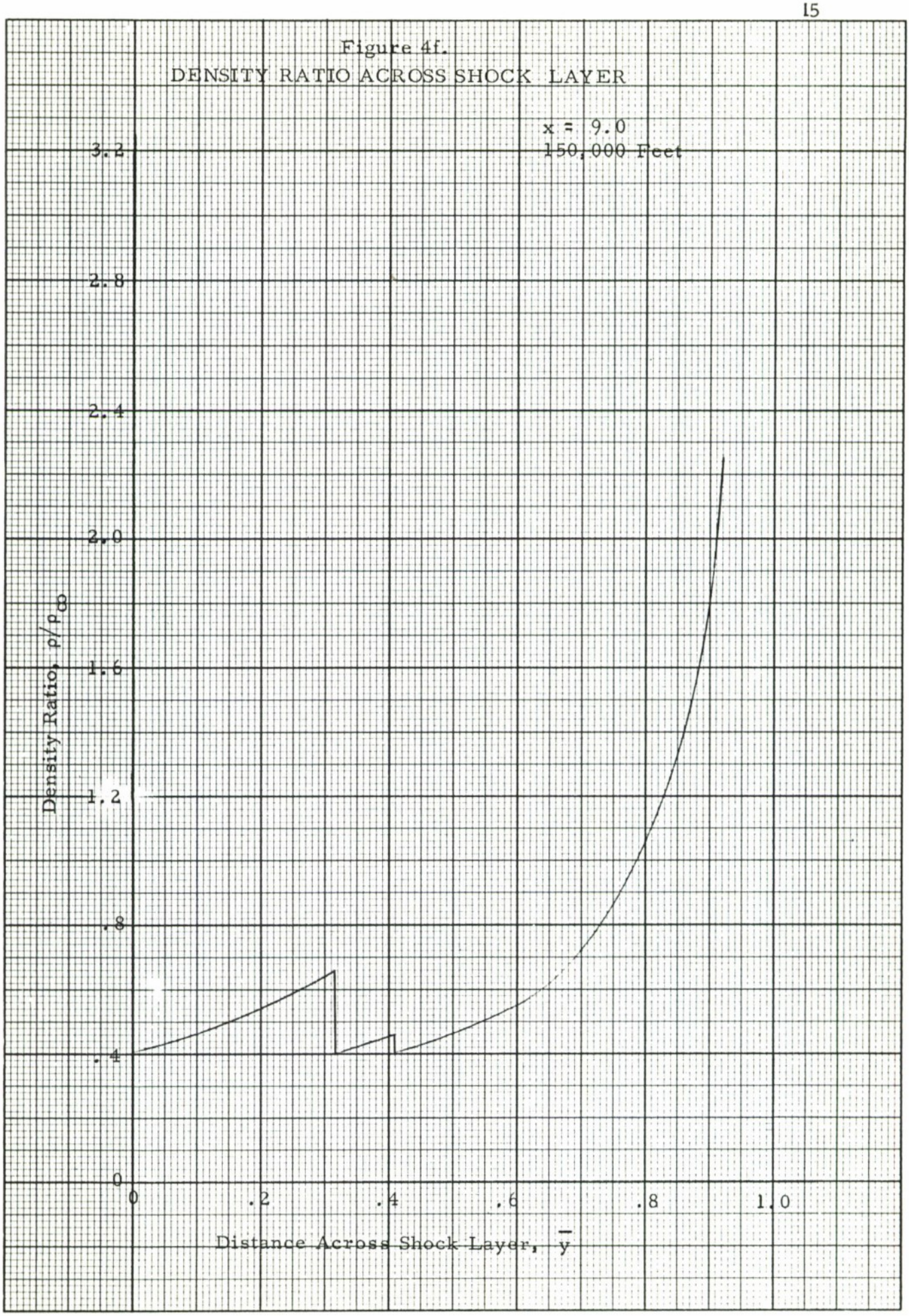

Figure 4g.

TEMPERATURE DISTRIBUTION ACROSS SHOCK LAYER

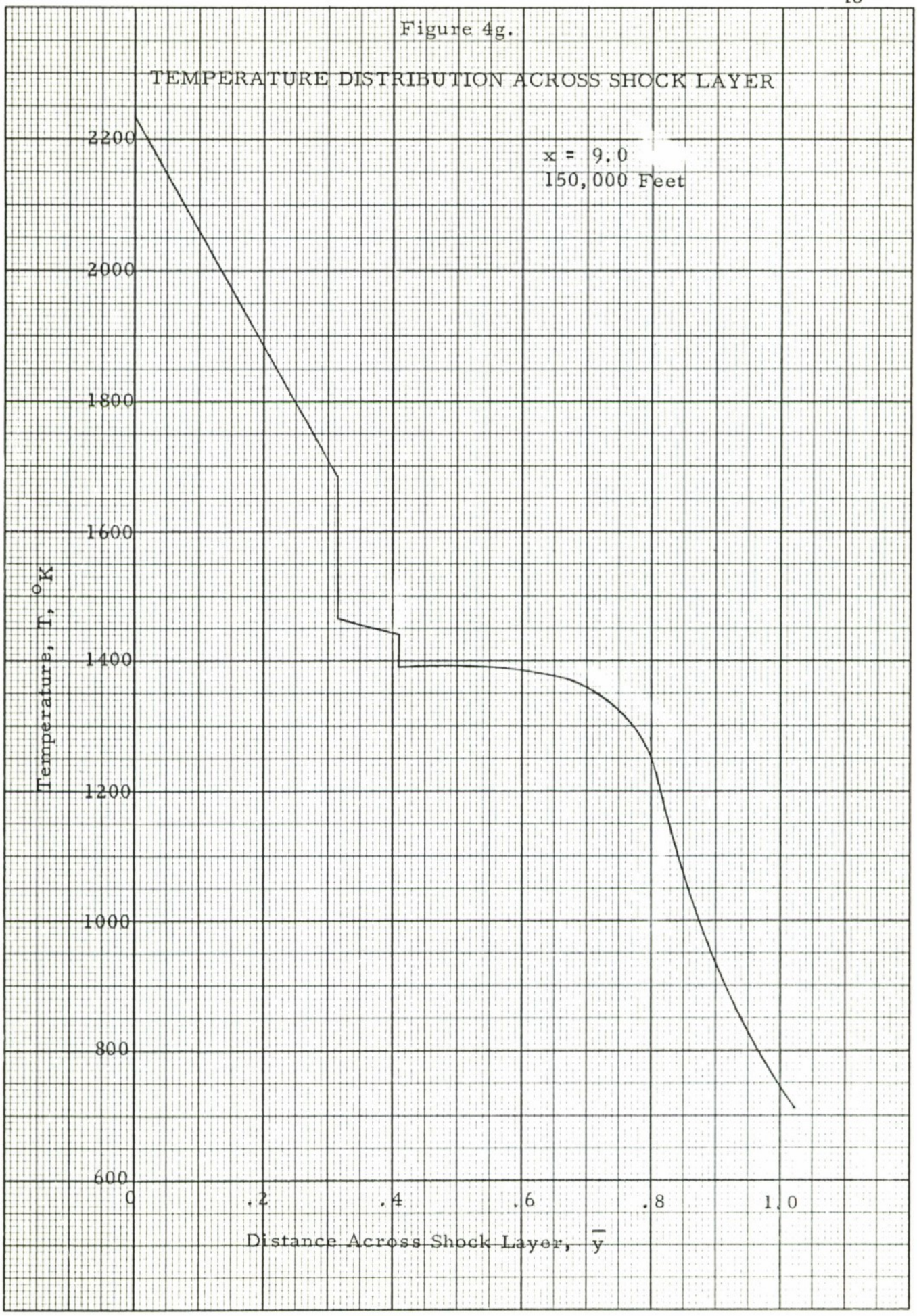

Figure 4h.

ELECTRON DENSITY DISTRIBUTION ACROSS SHOCK LAYER

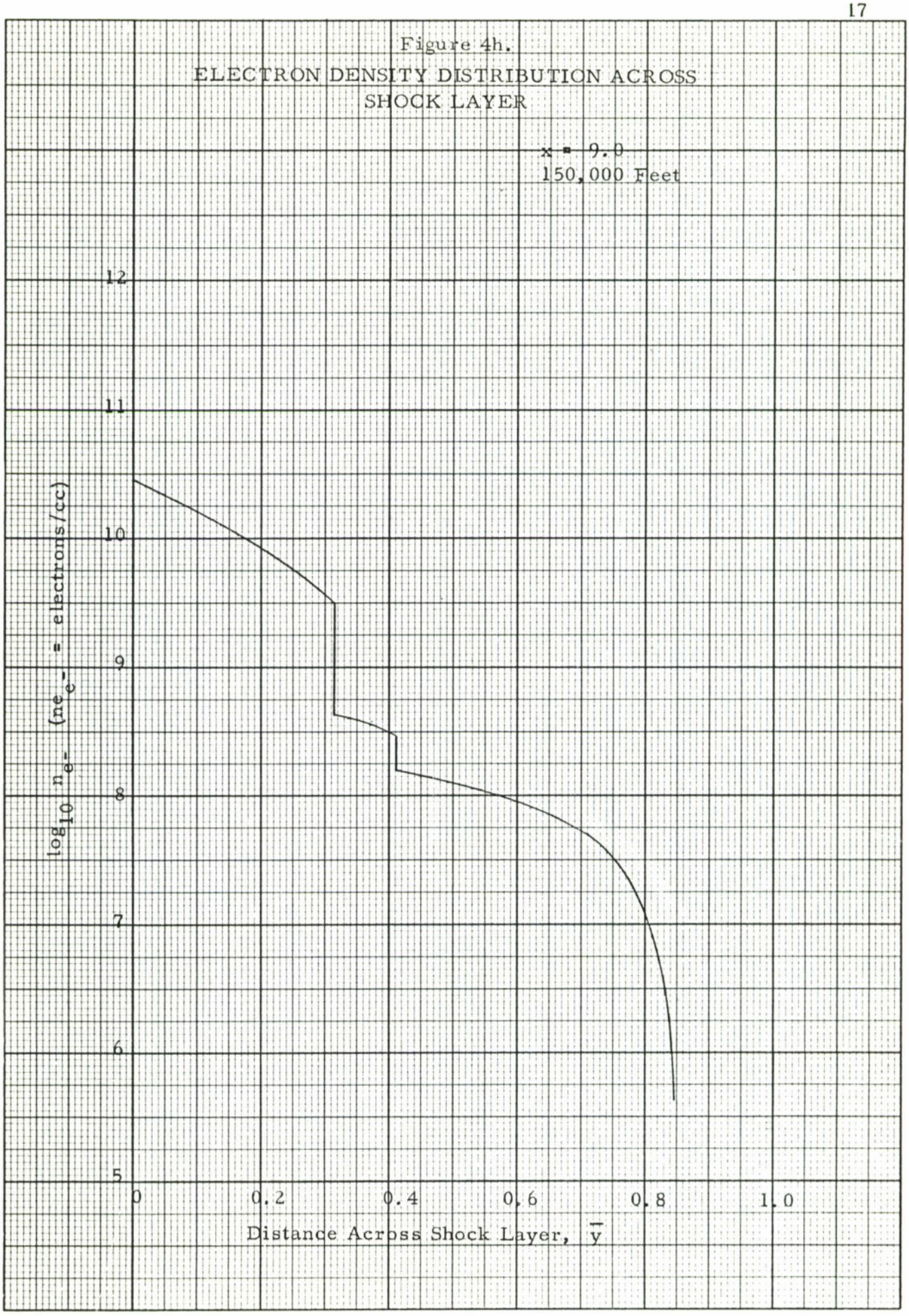

Figure 4i.

Pressure Ratio Across Shock Layer

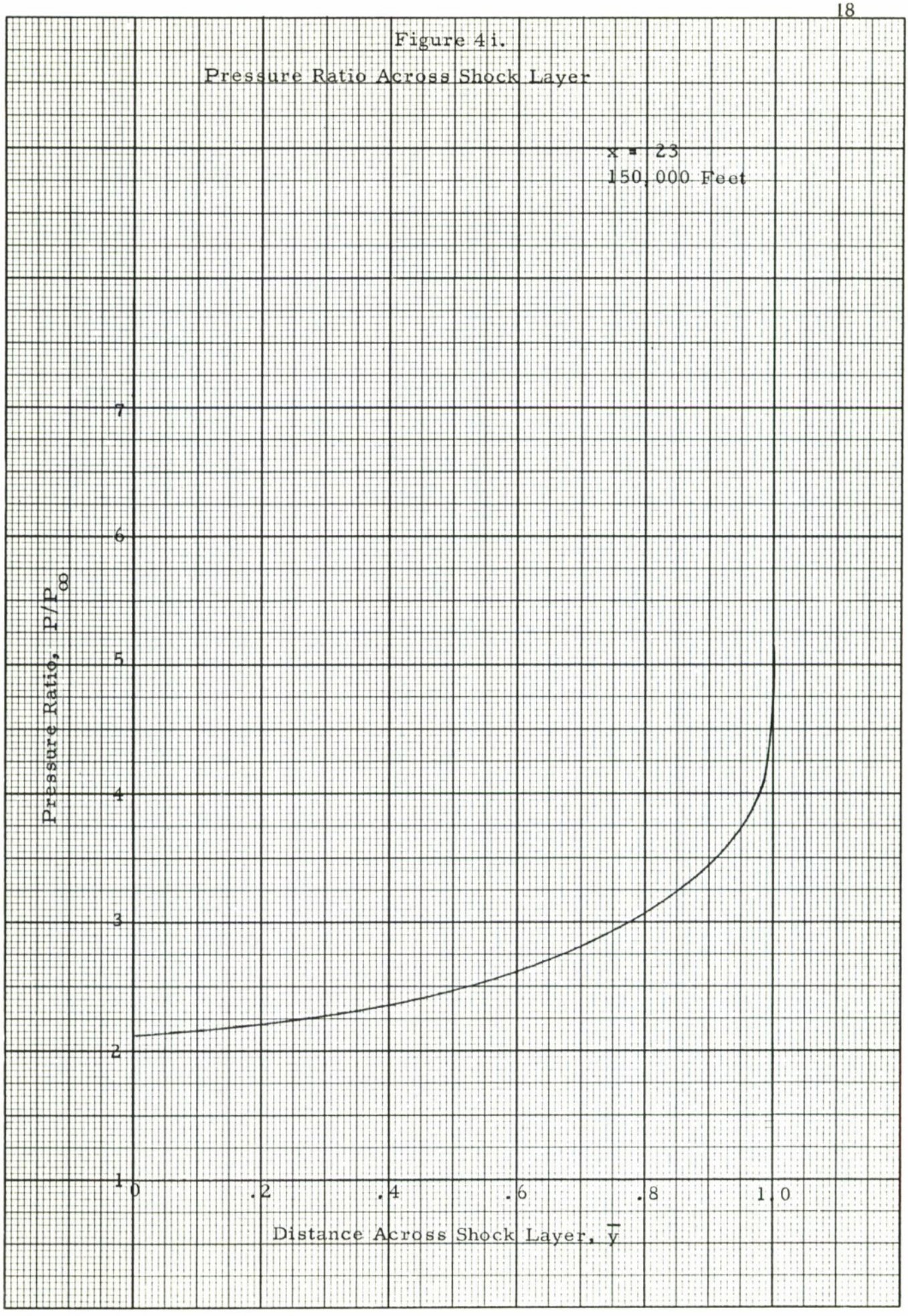

Figure 4j.
Density Ratio Across Shock Layer

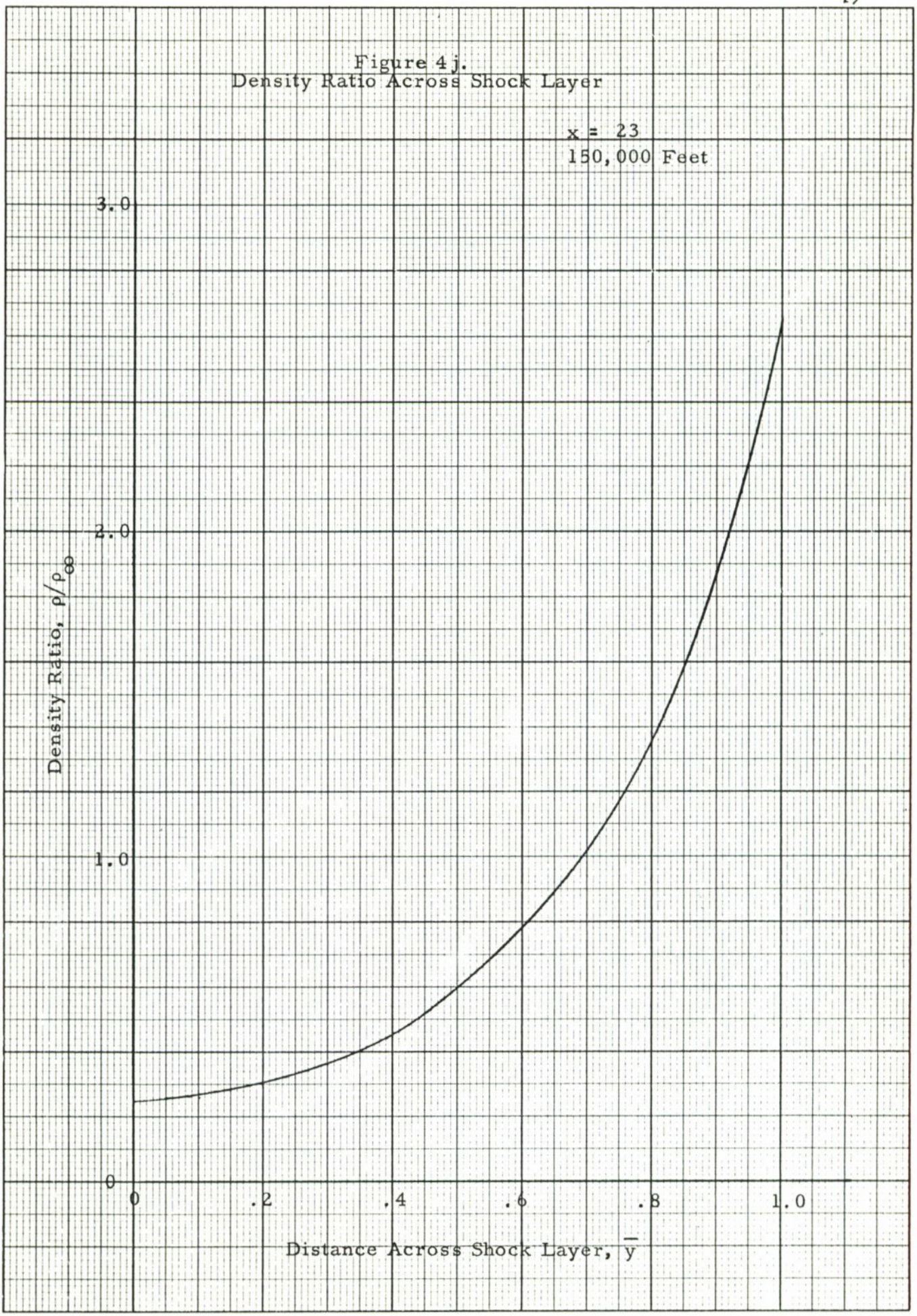

Figure 4k.

TEMPERATURE DISTRIBUTION ACROSS SHOCK LAYER

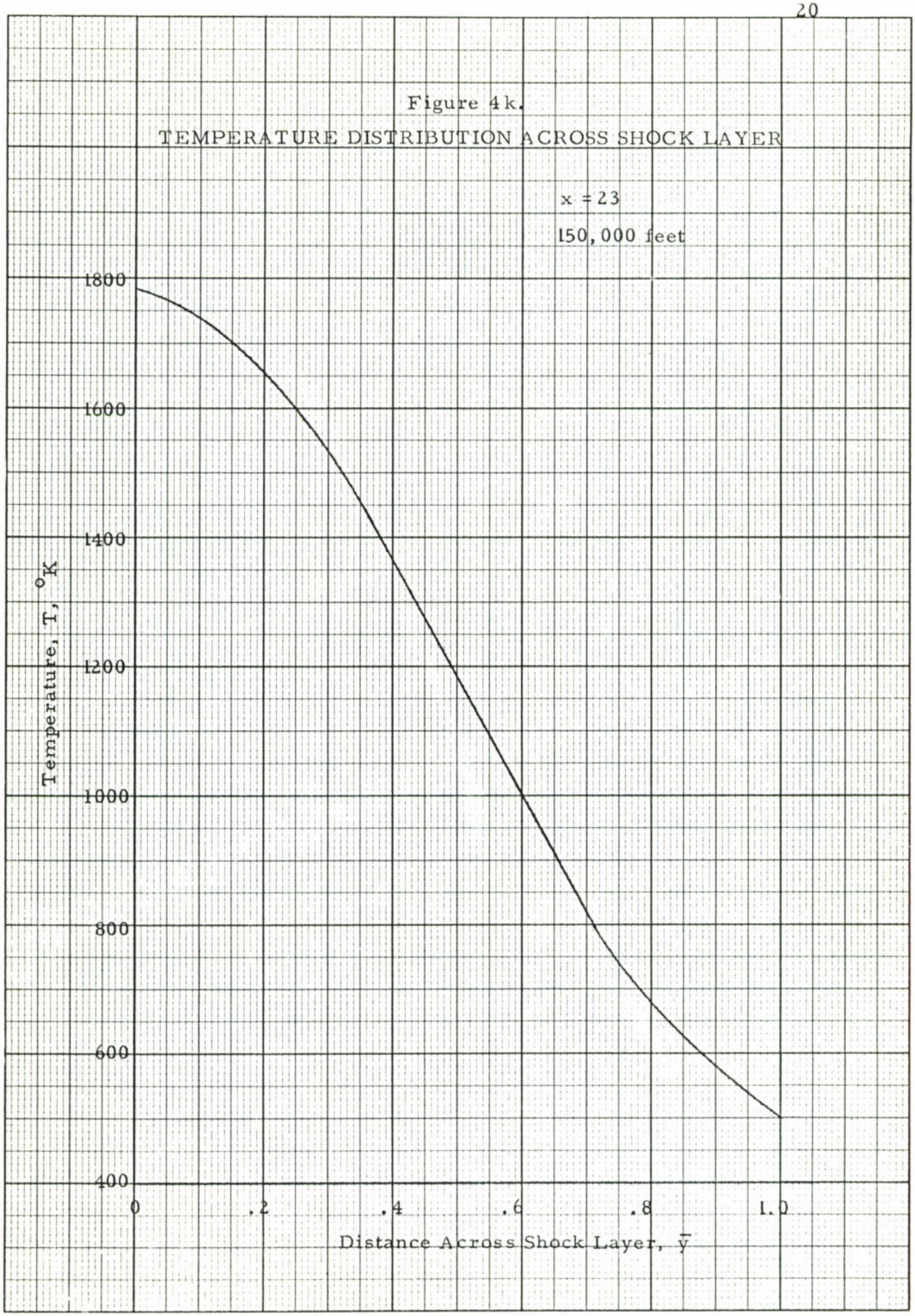

Figure 4 ℓ.

ELECTRON DENSITY DISTRIBUTION ACROSS SHOCK LAYER

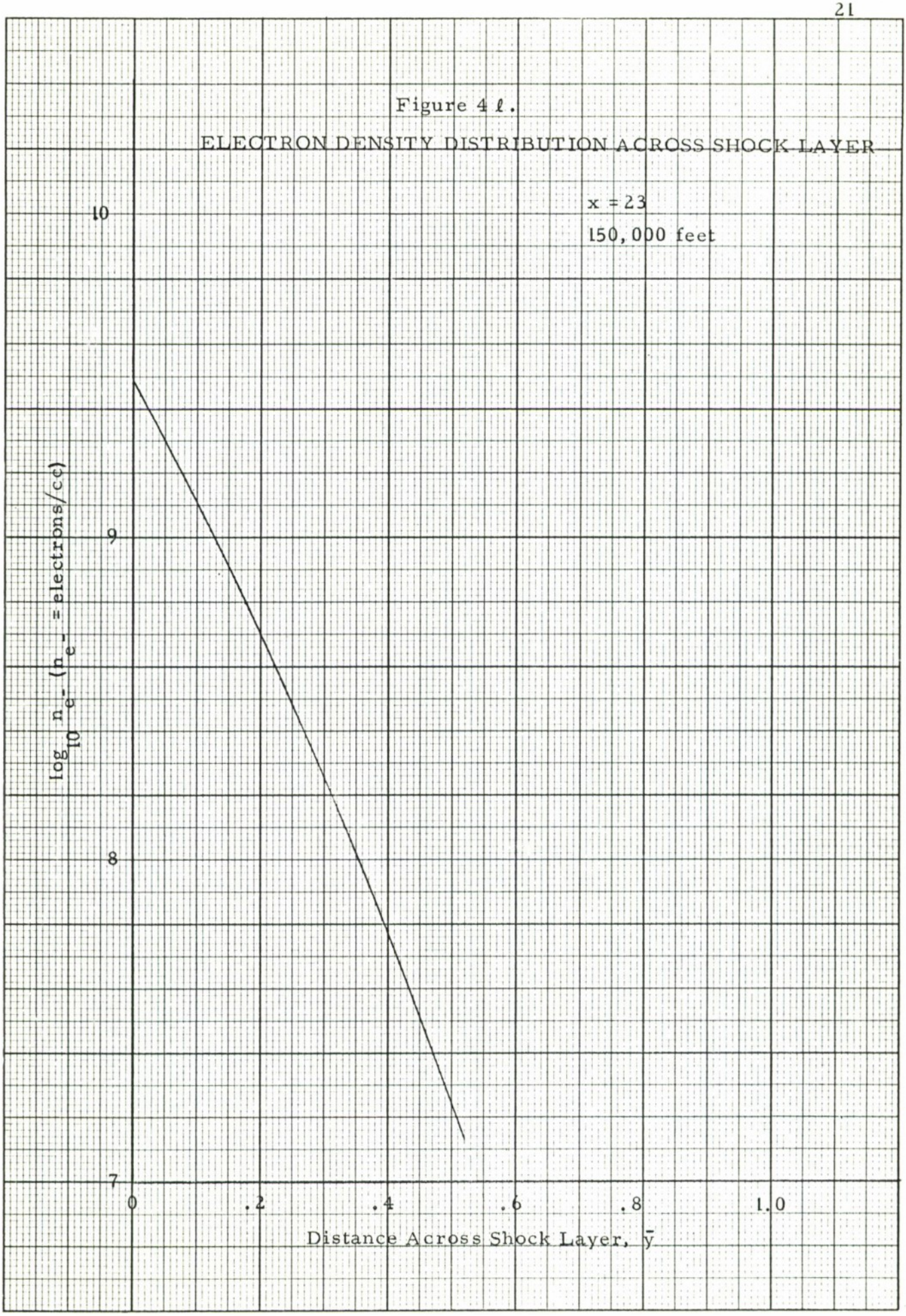

Figure 5a
PRESSURE RATIO ACROSS SHOCK LAYER
200,000 feet

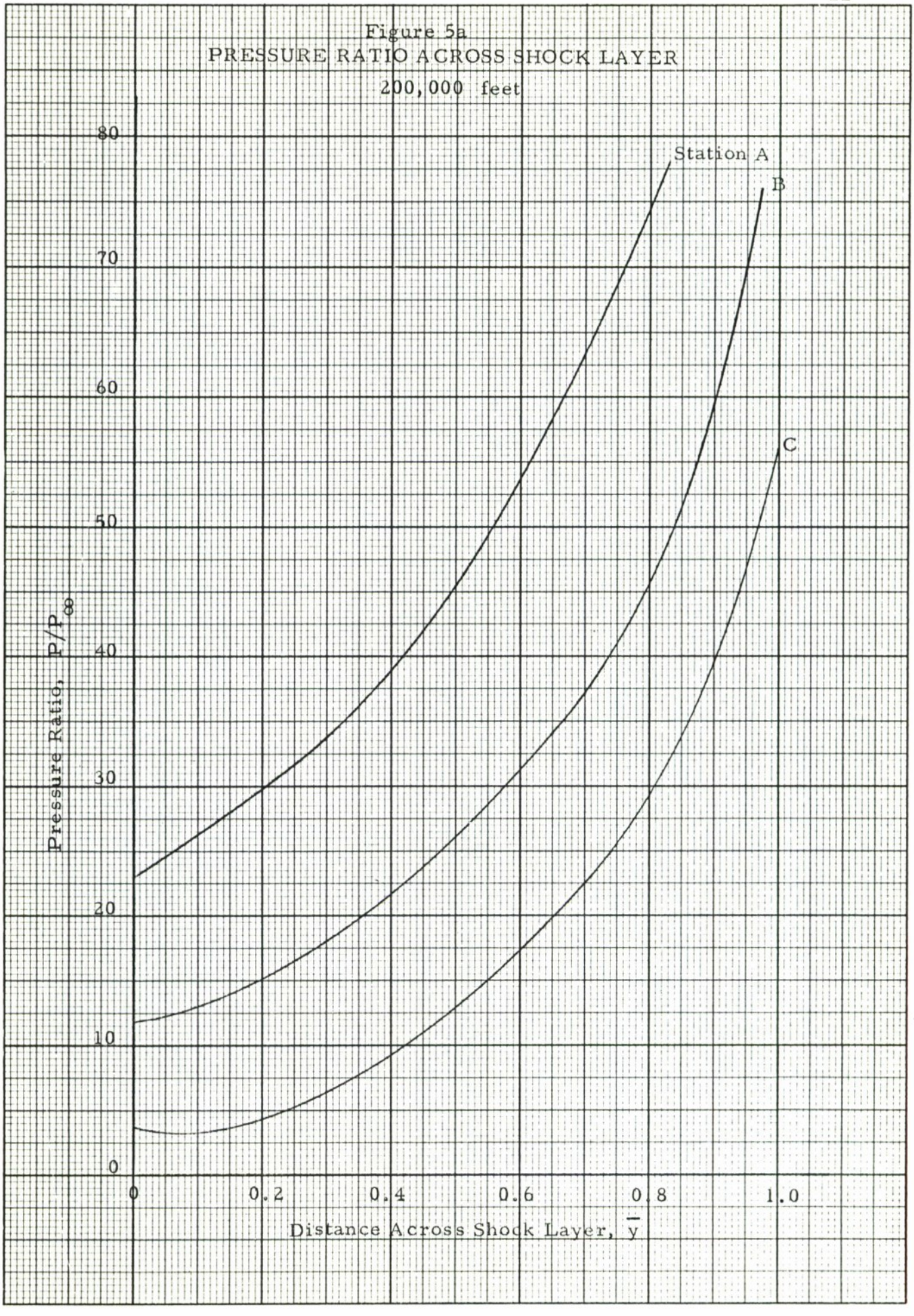

Figure 5b
DENSITY RATIO ACROSS SHOCK LAYER
200,000 feet

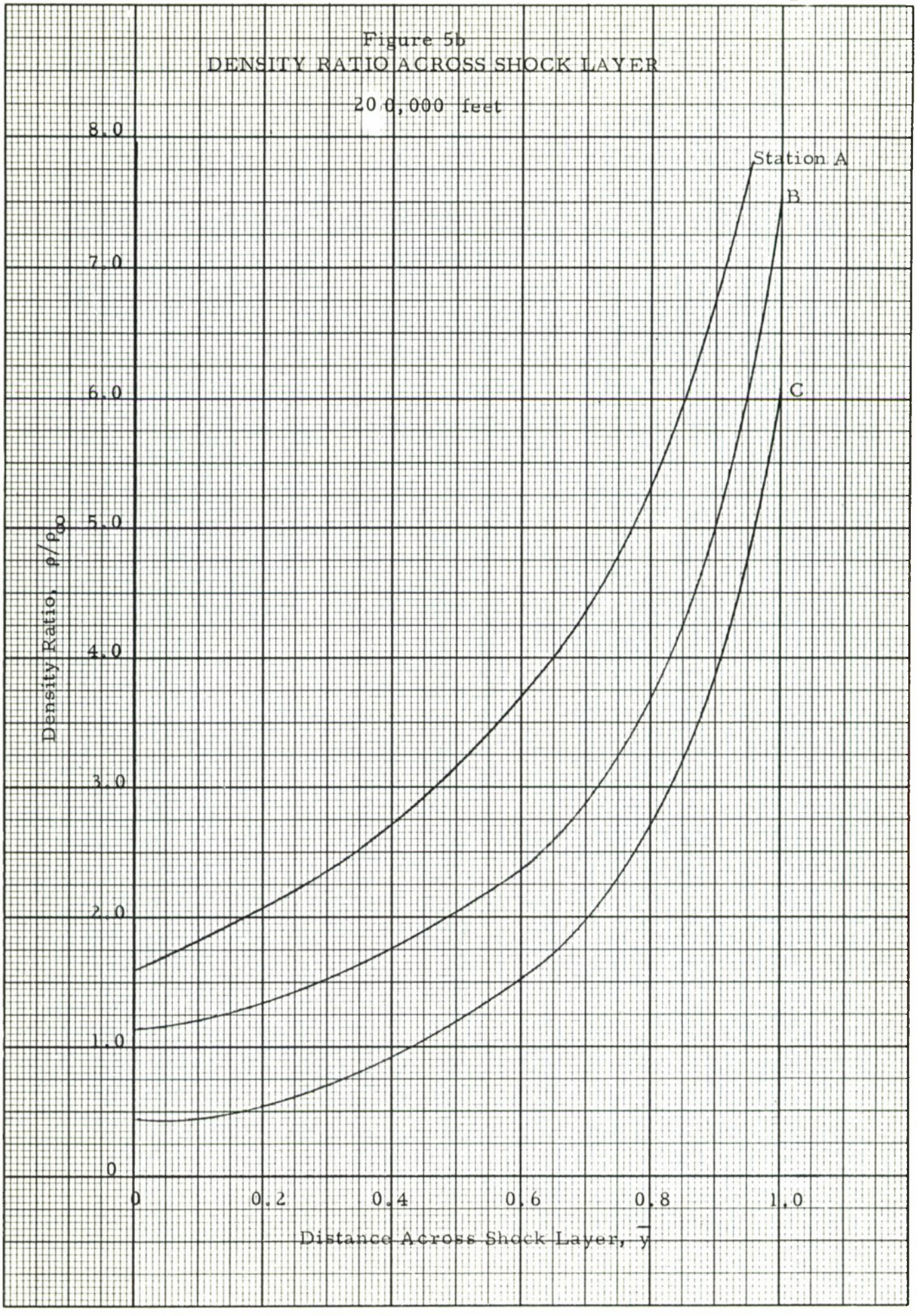

Figure 5c
TEMPERATURE DISTRIBUTION ACROSS SHOCK LAYER
200,000 feet

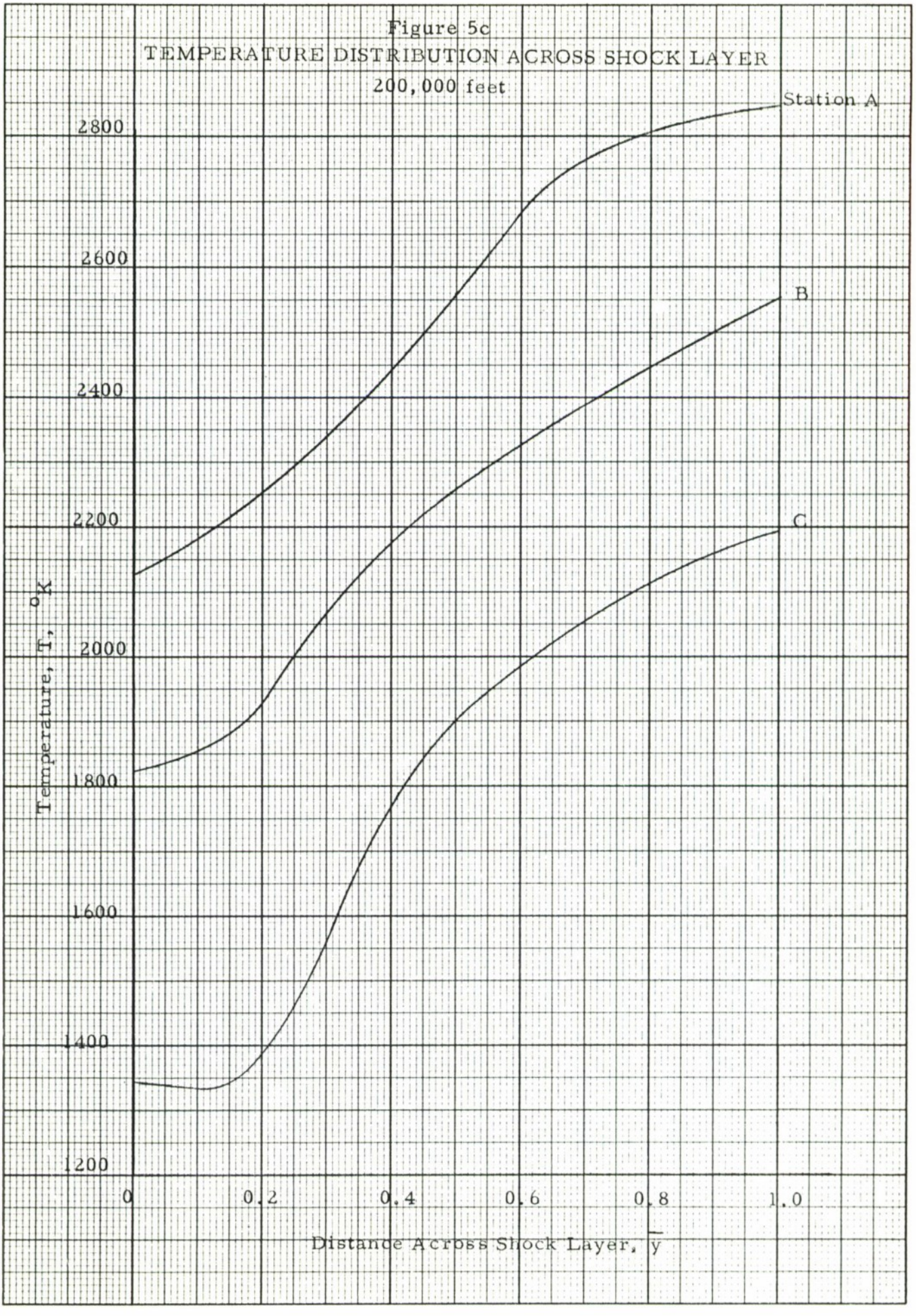

Figure 5d
ELECTRON DENSITY DISTRIBUTION ACROSS SHOCK LAYER
200,000 Feet

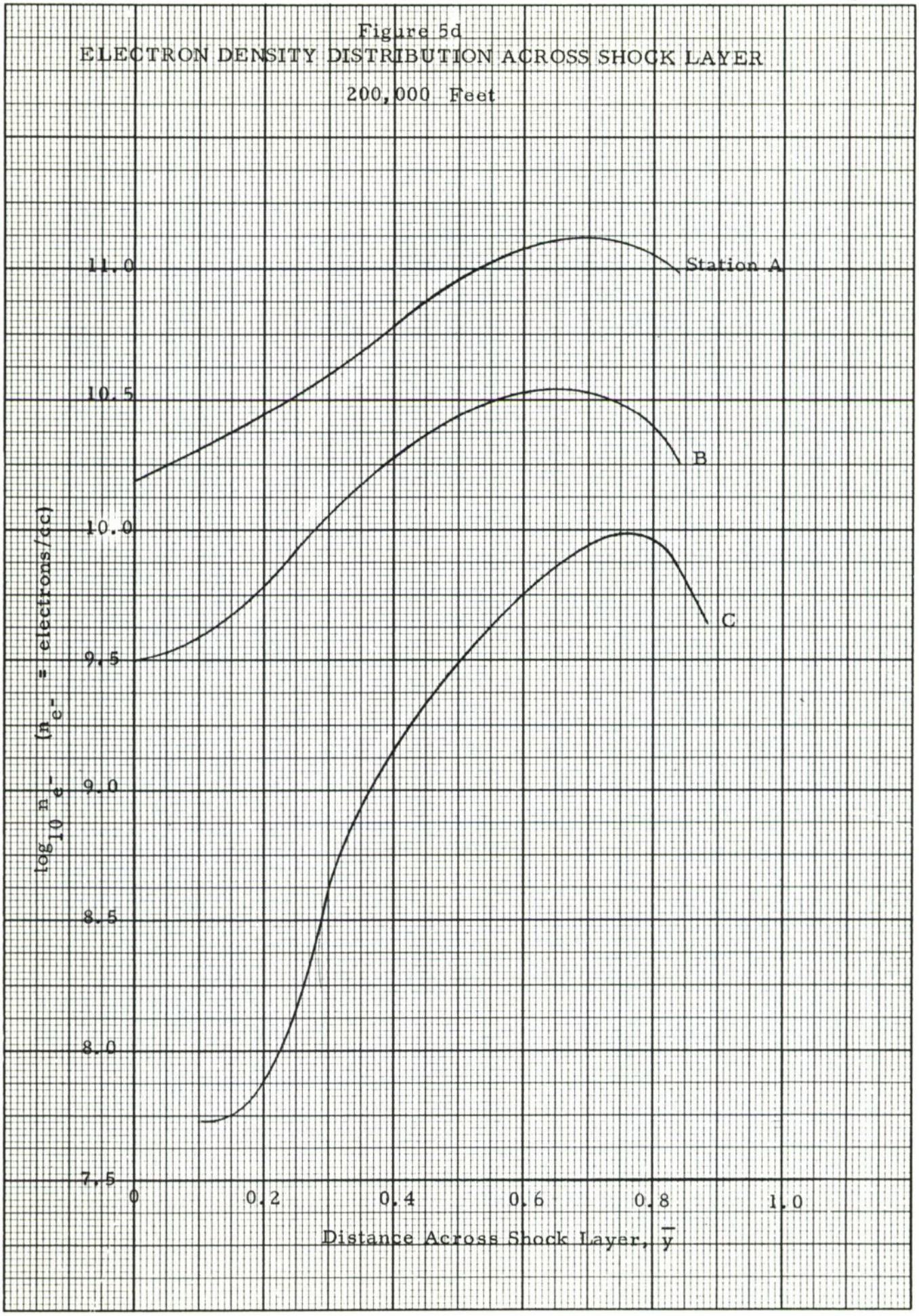

Figure 5e
Pressure Ratio Across Shock Layer

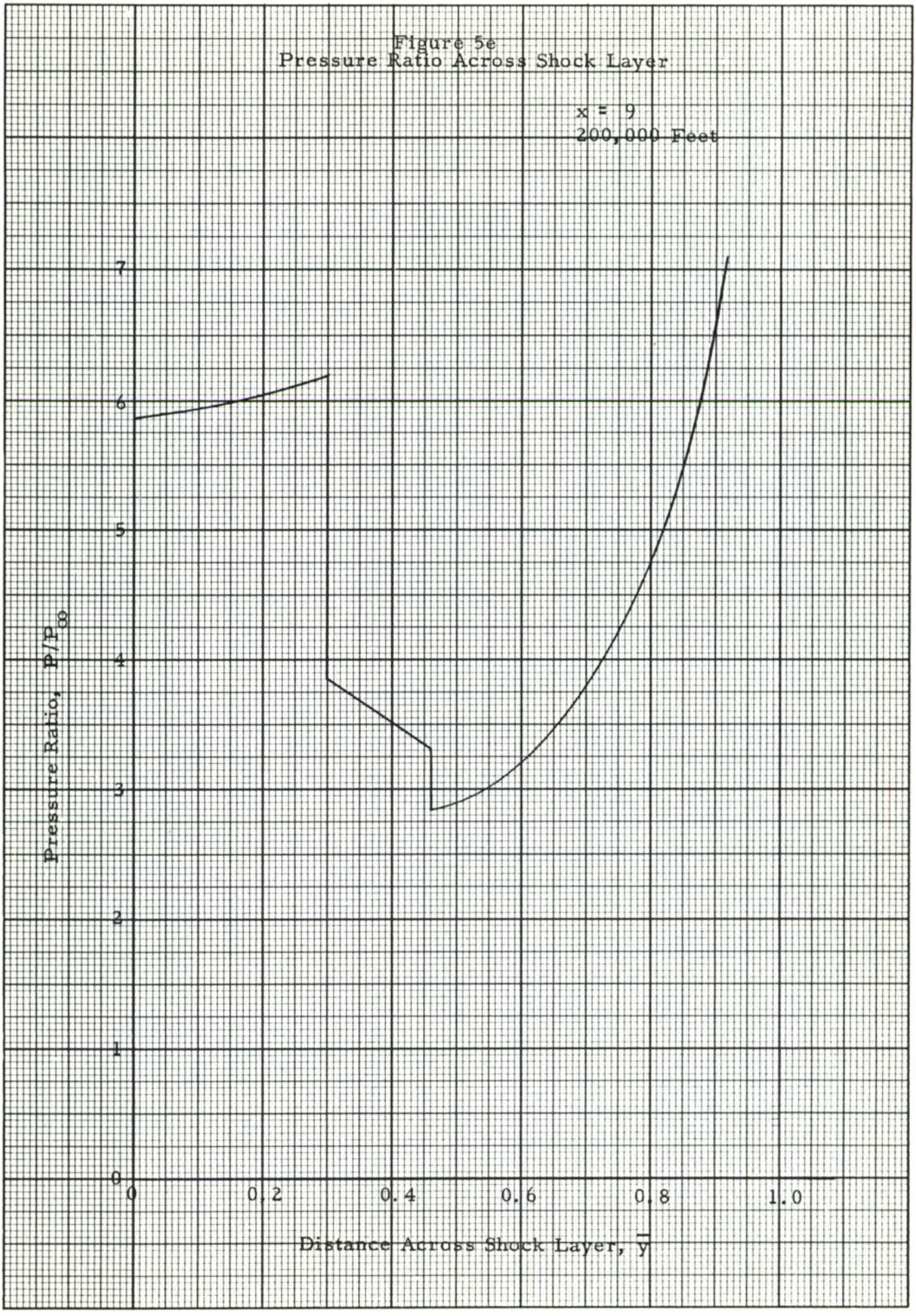

Figure 5f
Density Ratio Across Shock Layer

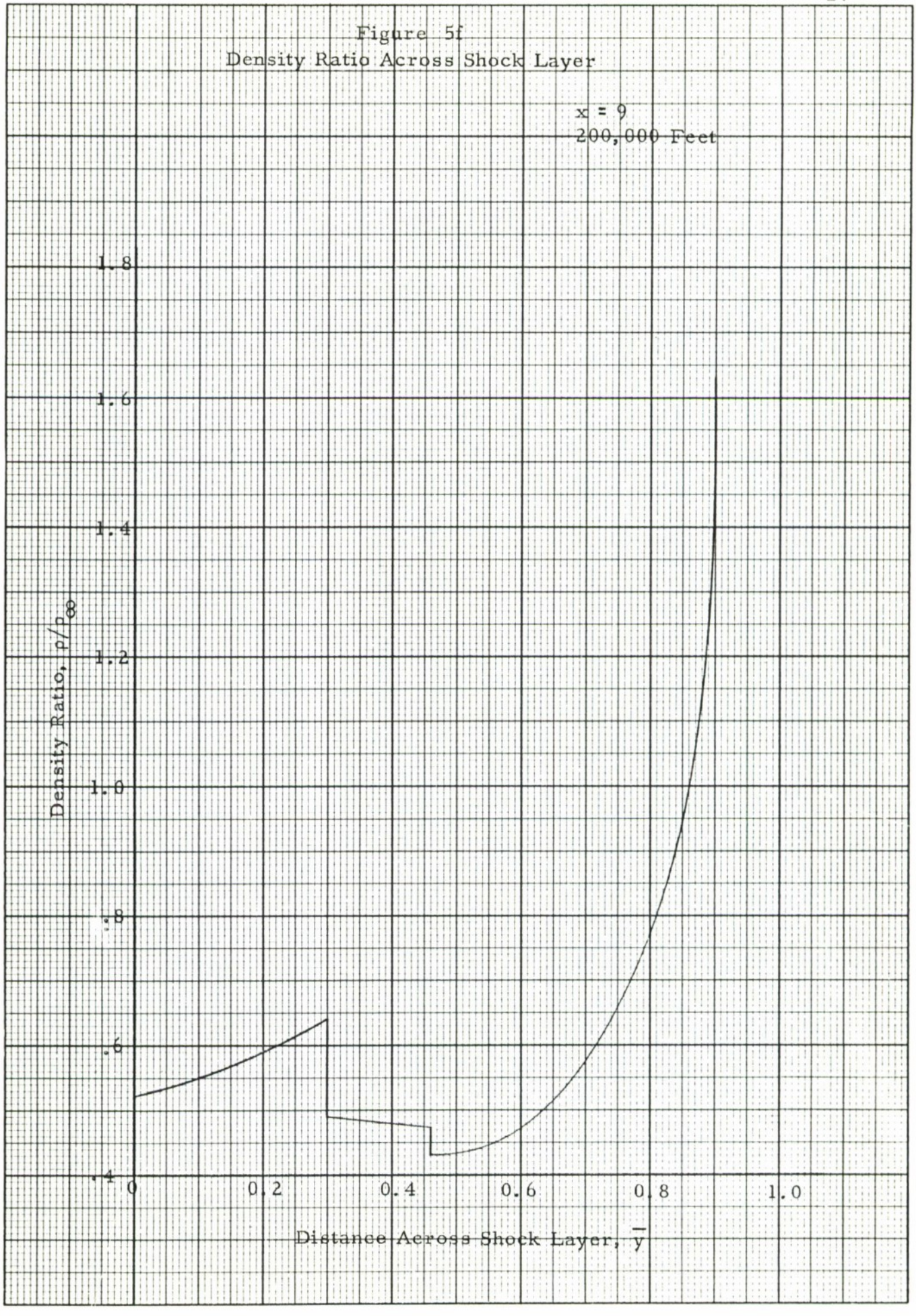

Figure 5g.

Temperature Distribution Across Shock Layer

x = 9

200,000 feet

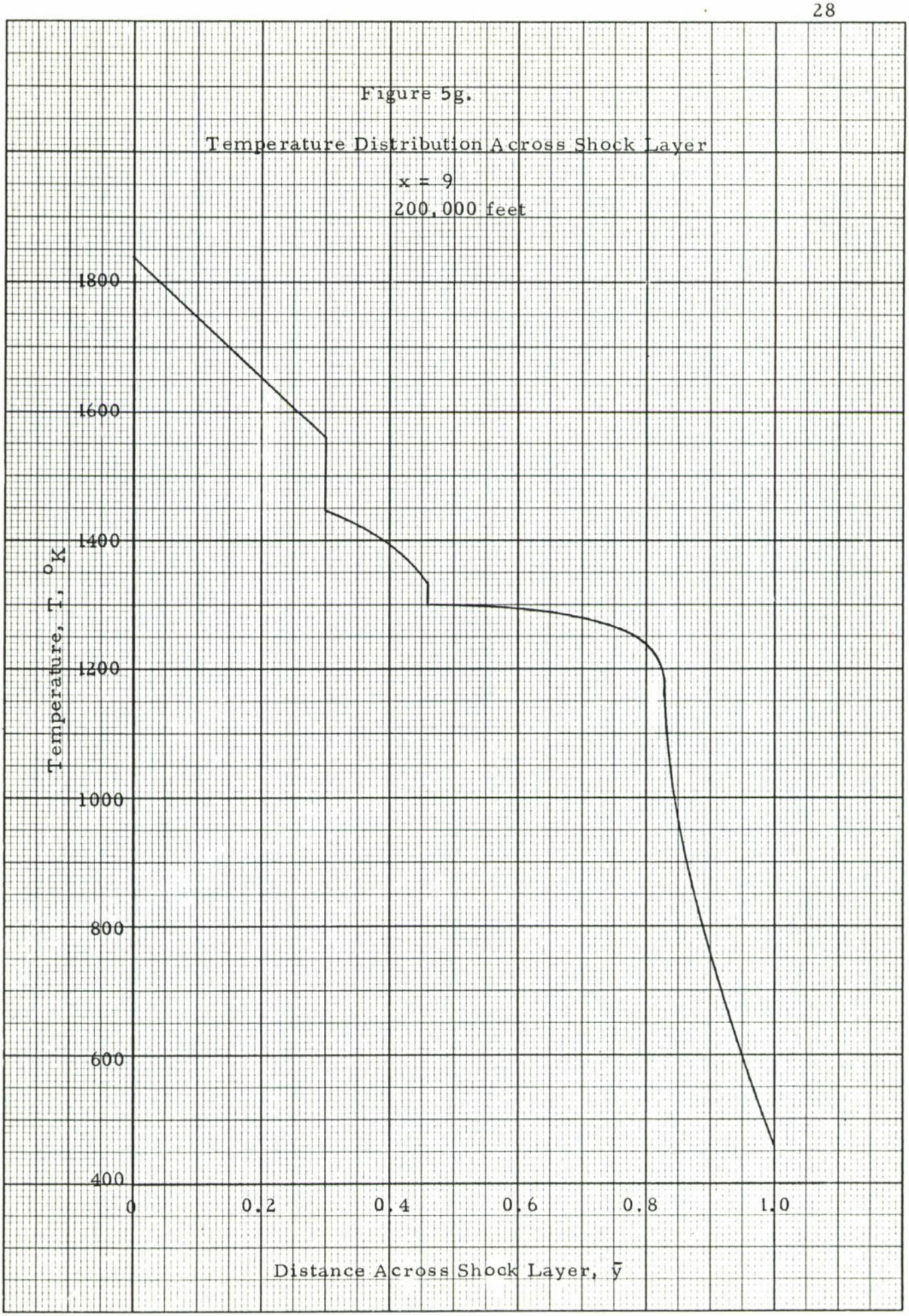

Figure 5h
Electron Density Distribution Across Shock Layer

x = 9
200,000 Feet

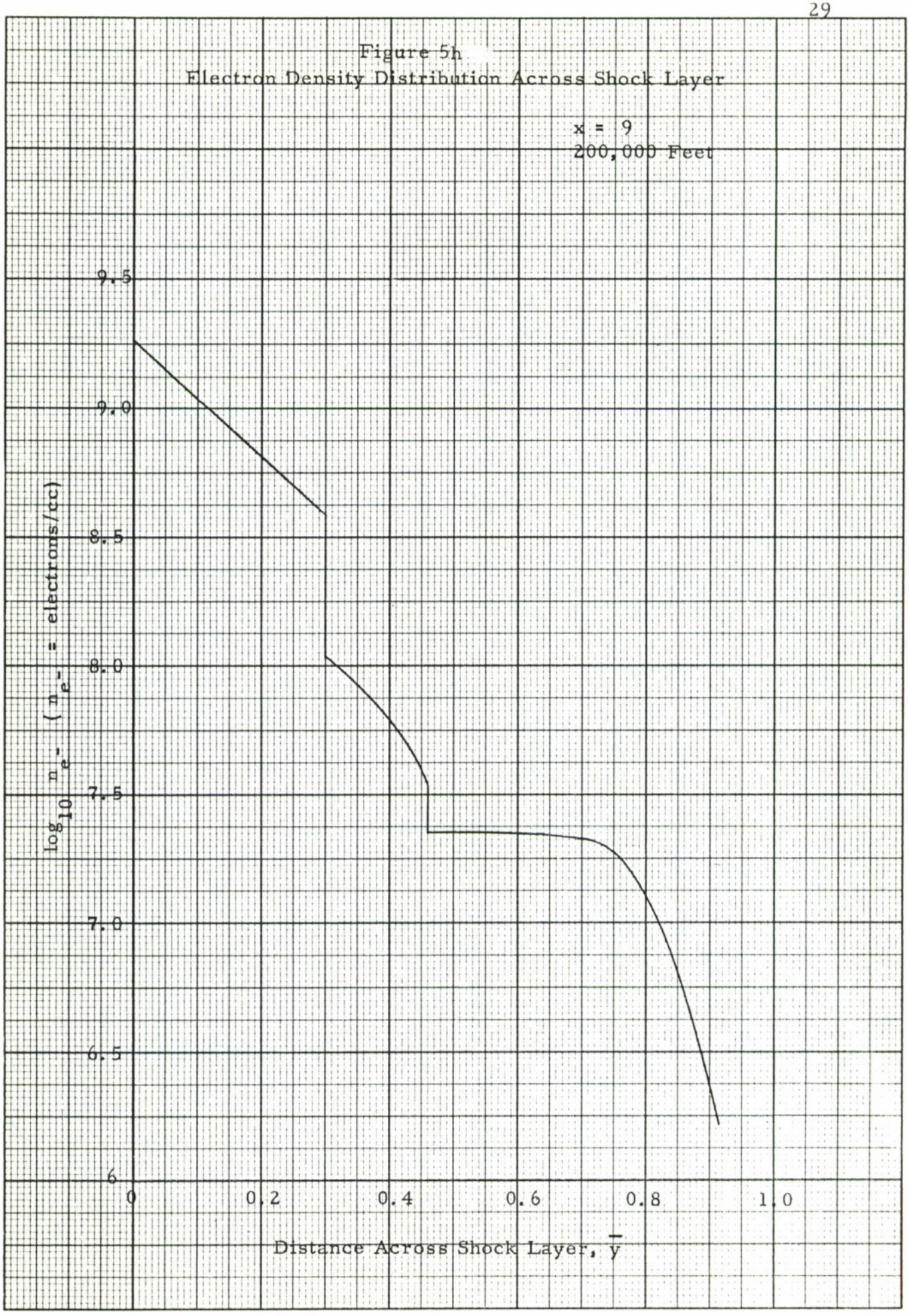

Figure 5i
Pressure Ratio Across Shock Layer

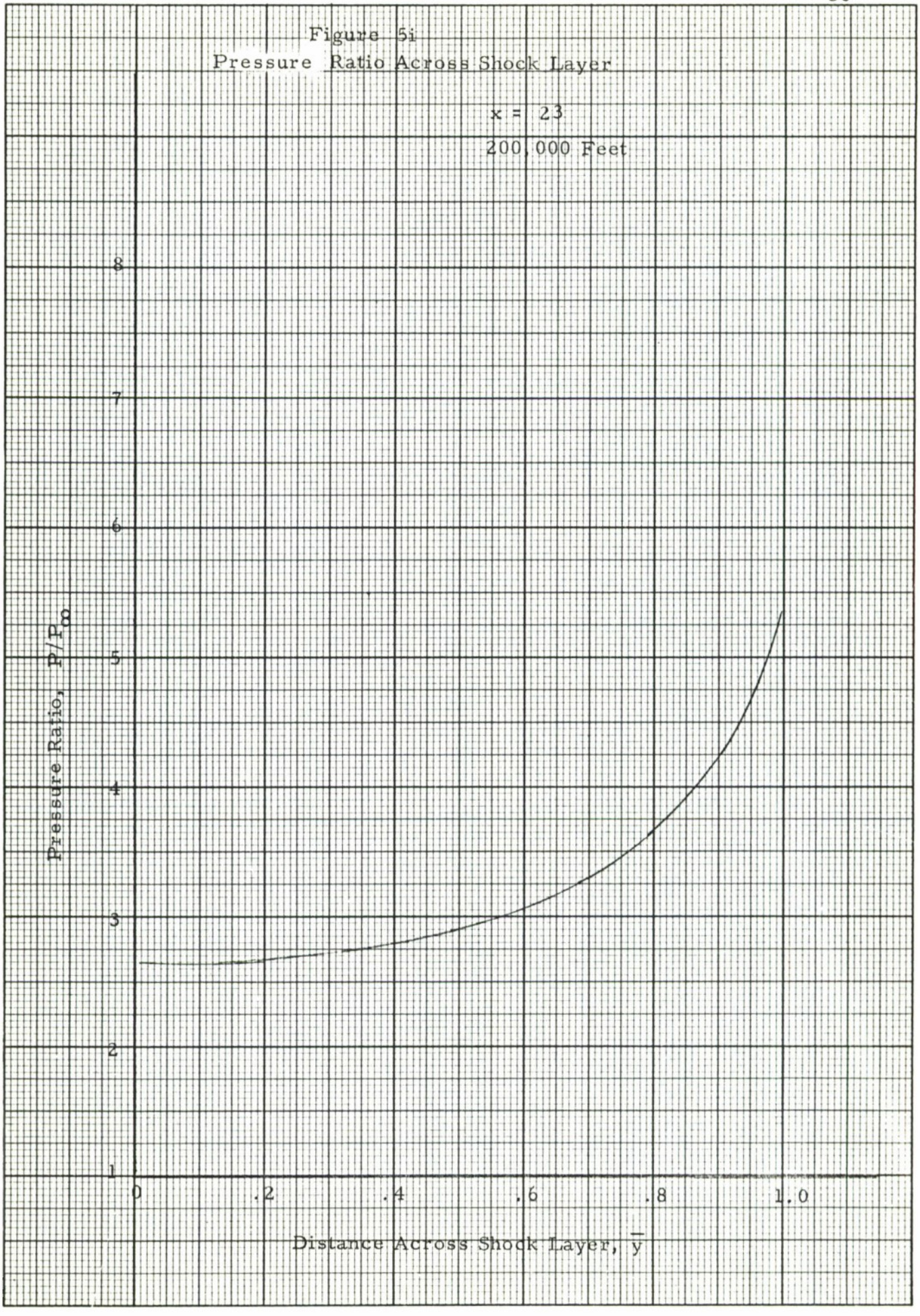

Figure 5j
Density Ratio Across Shock Layer

x = 23

200,000 Feet

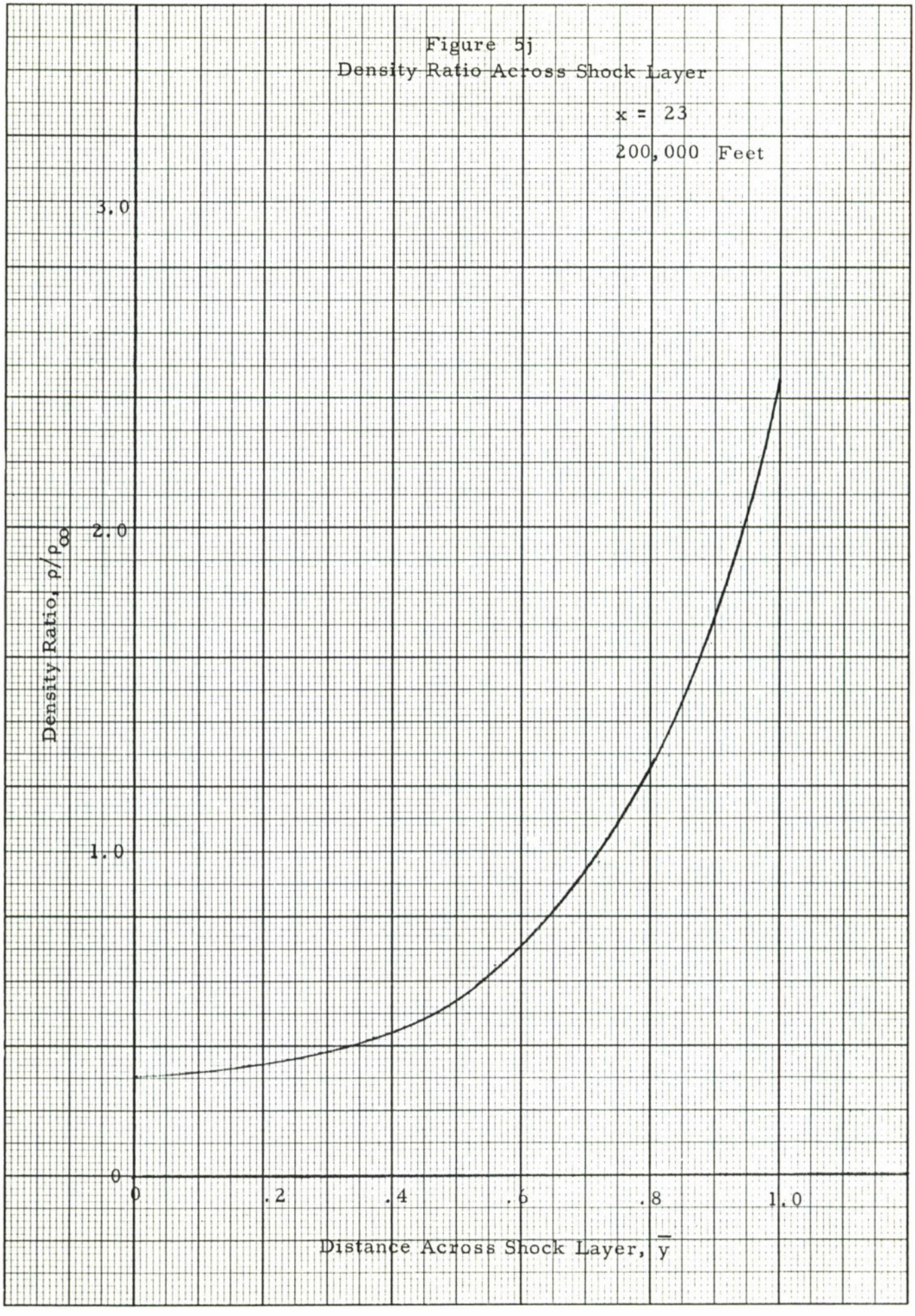

Figure 5k
Temperature Distribution Across Shock Layer

x = 23
200,000 Feet

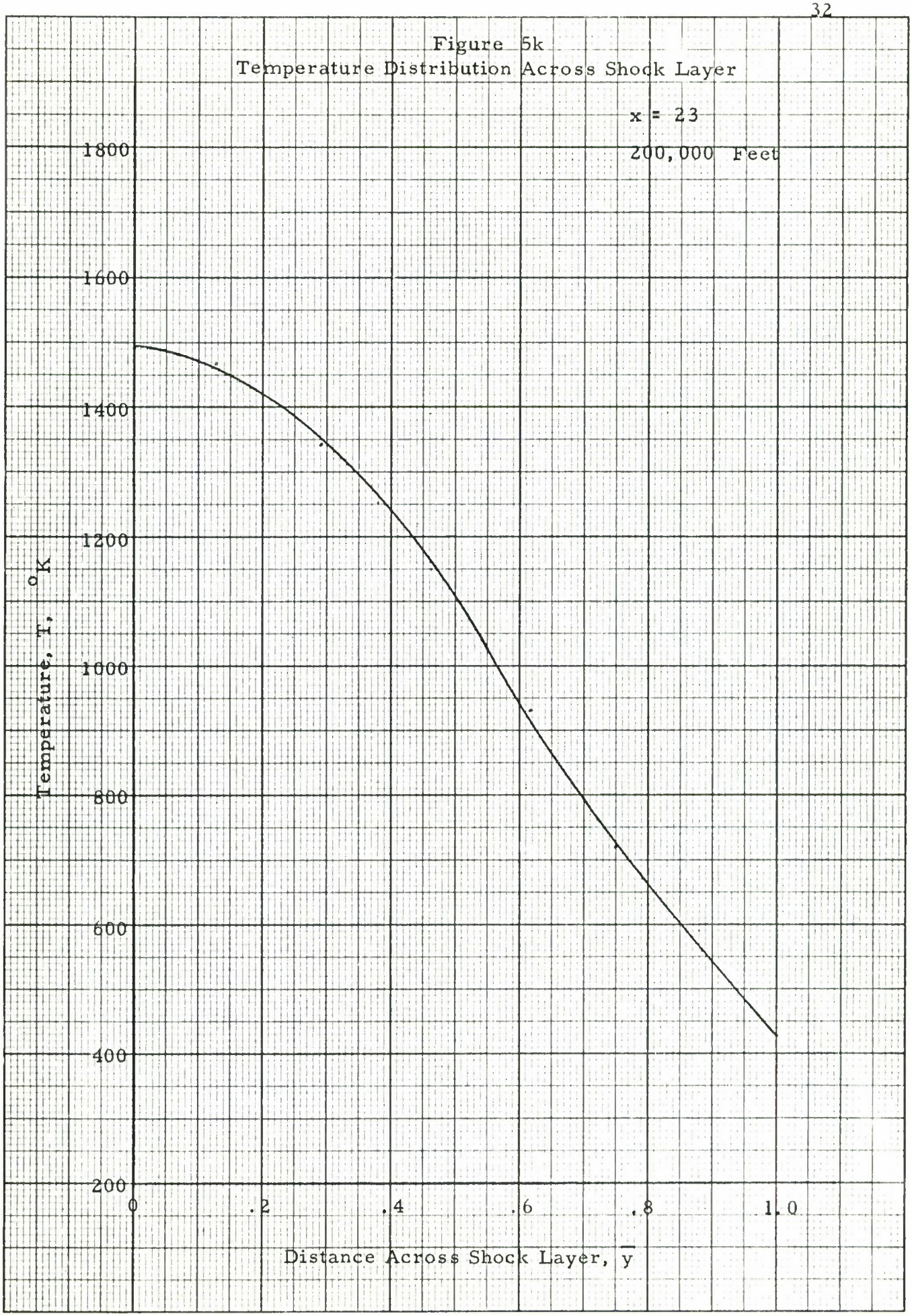

Figure 5ℓ.

Electron Density Distribution Across Shock Layer

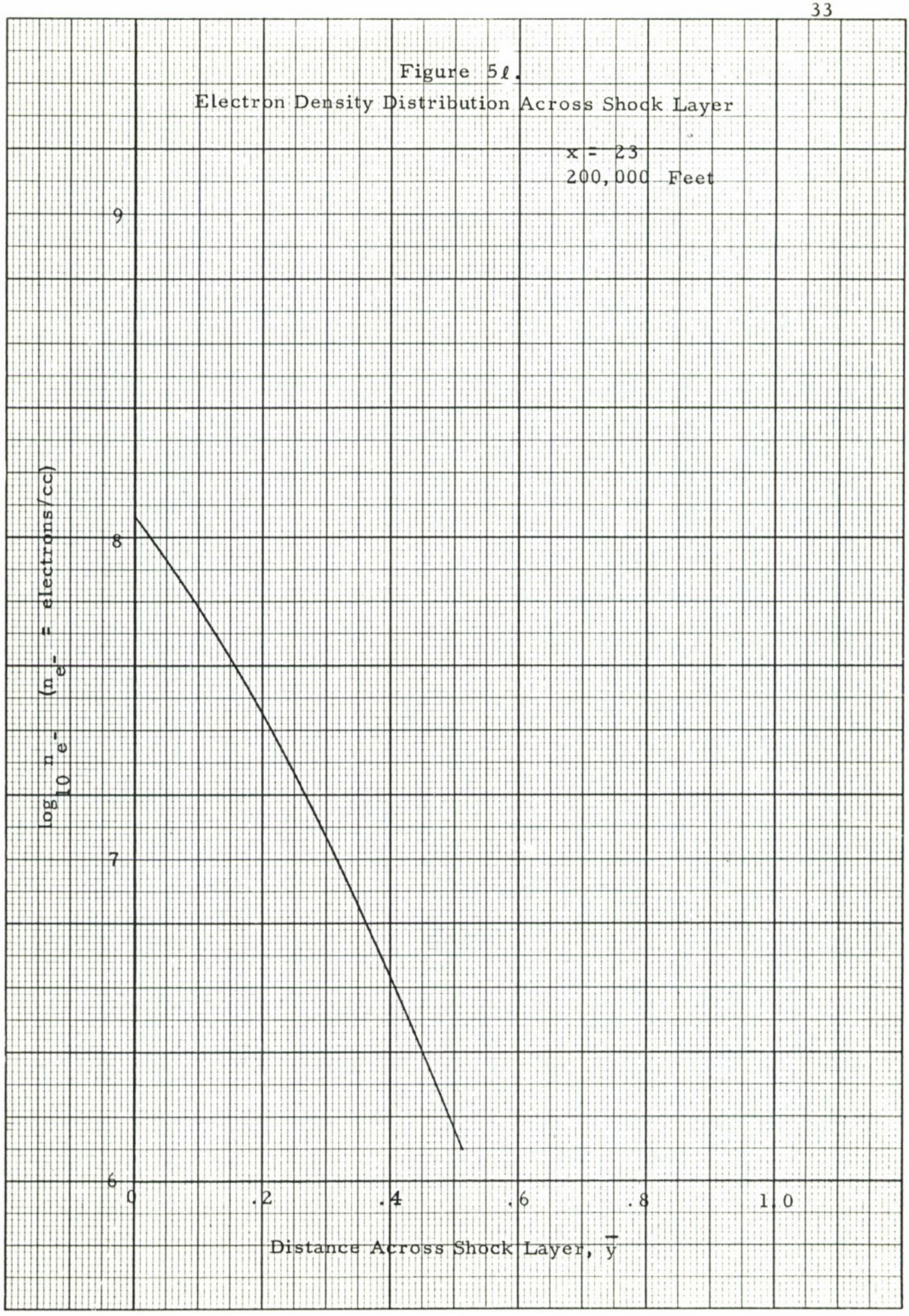

Figure 6a.
PRESSURE RATIO ACROSS SHOCK LAYER
250,000 feet

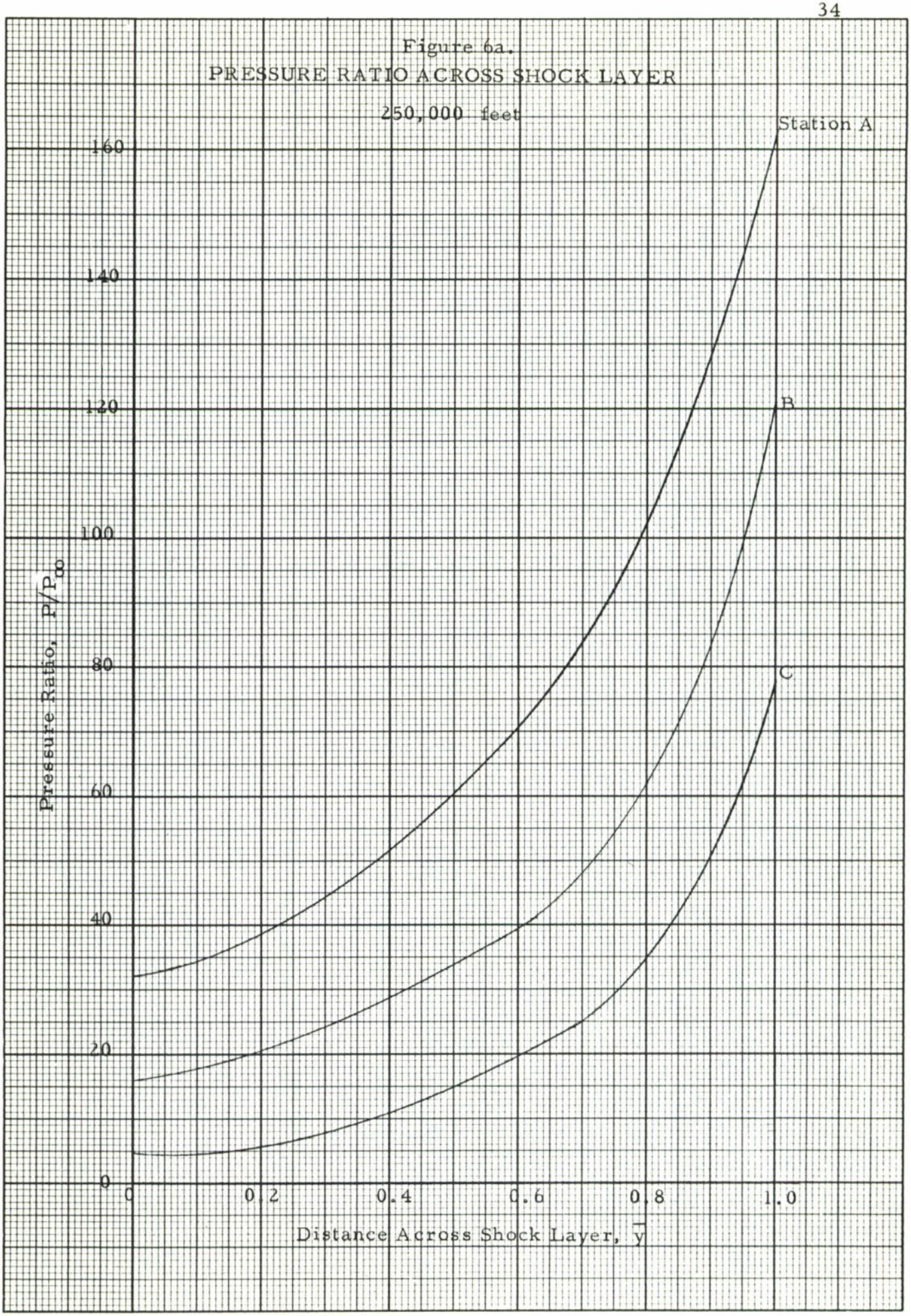

Figure 6b.
DENSITY RATIO ACROSS SHOCK LAYER
250,000 feet

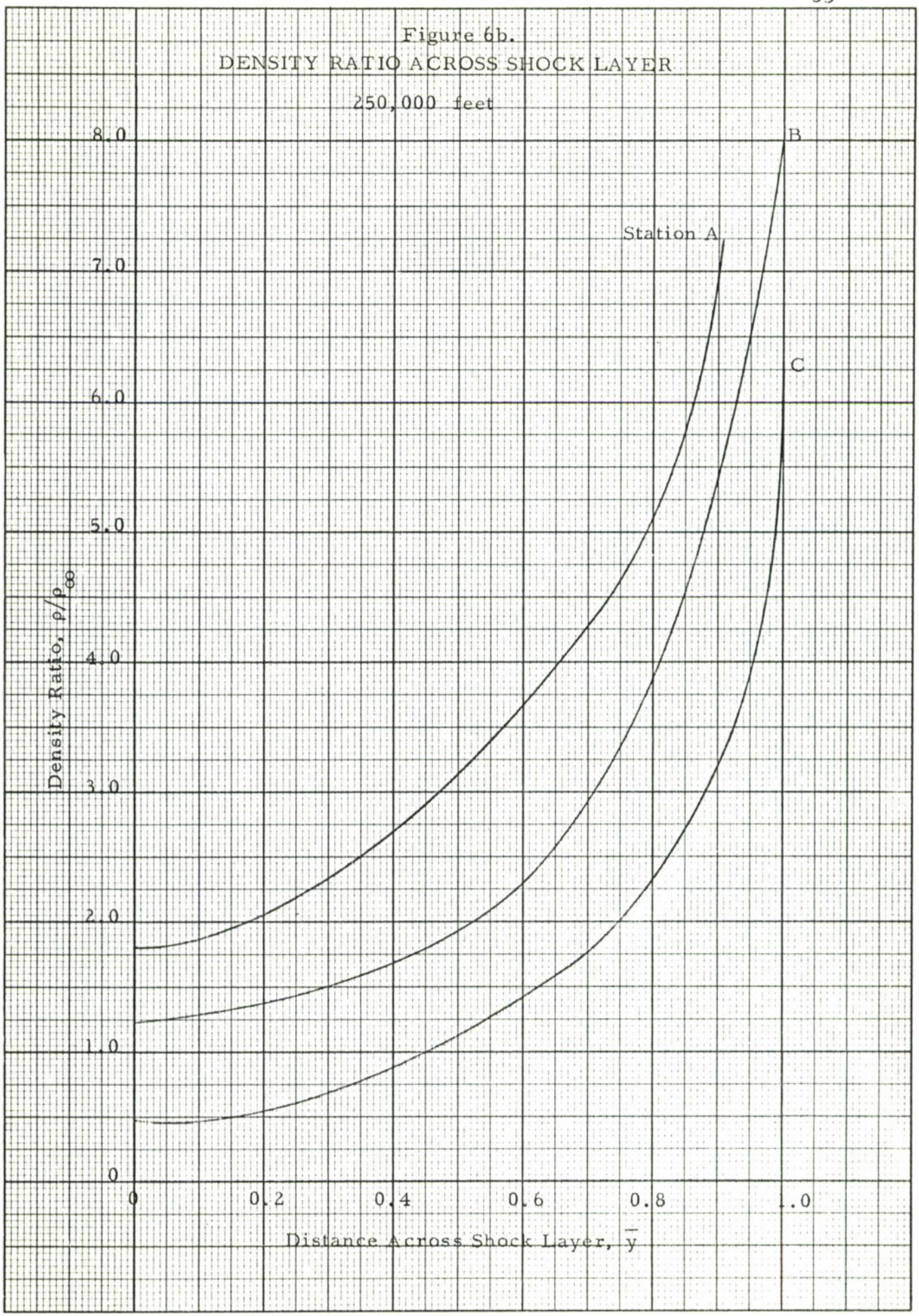

Figure 6c

Temperature Distribution Across Shock Layer

250,000 Feet

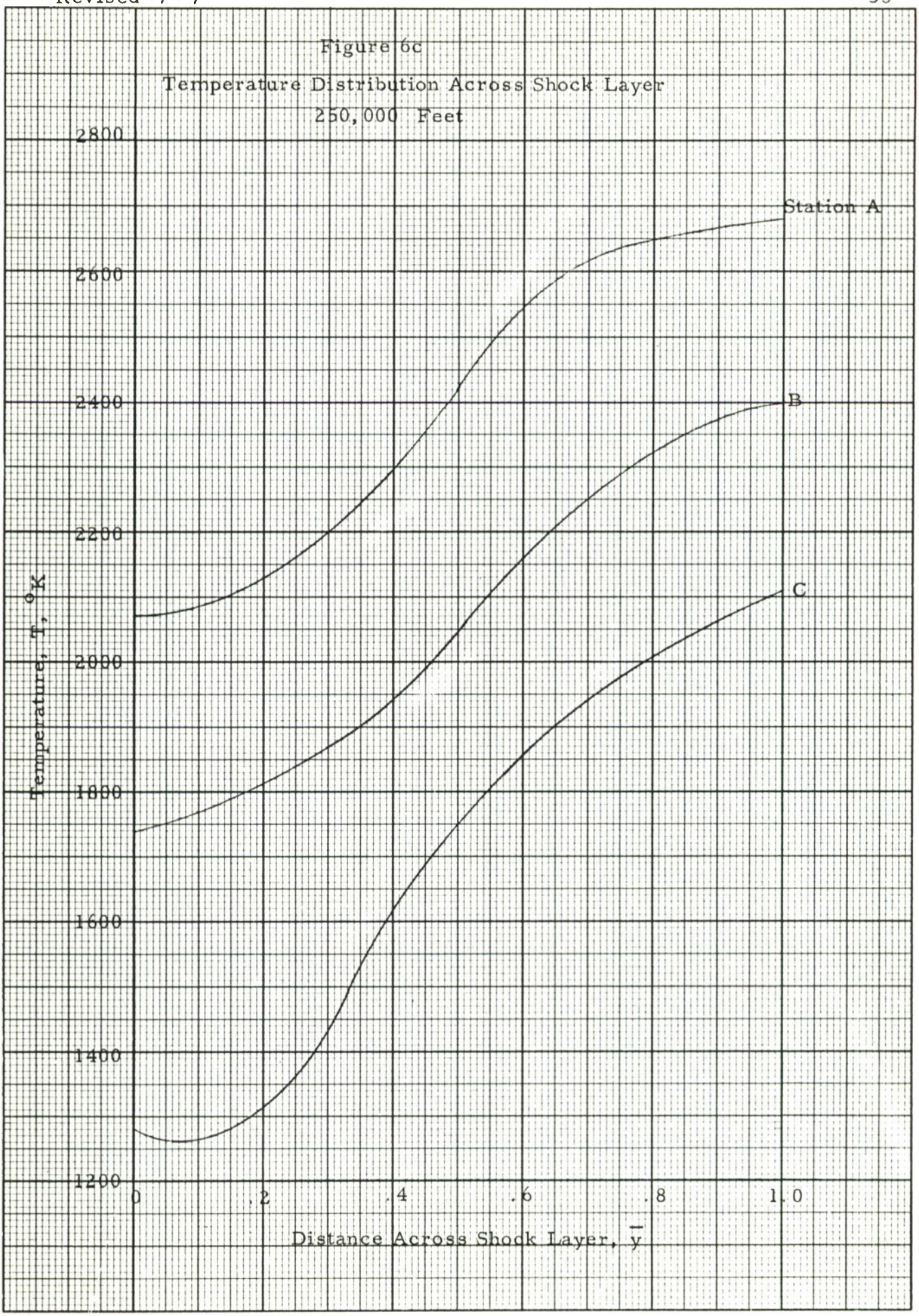

Figure 6d.
ELECTRON DENSITY DISTRIBUTION ACROSS SHOCK LAYER
250,000 Feet

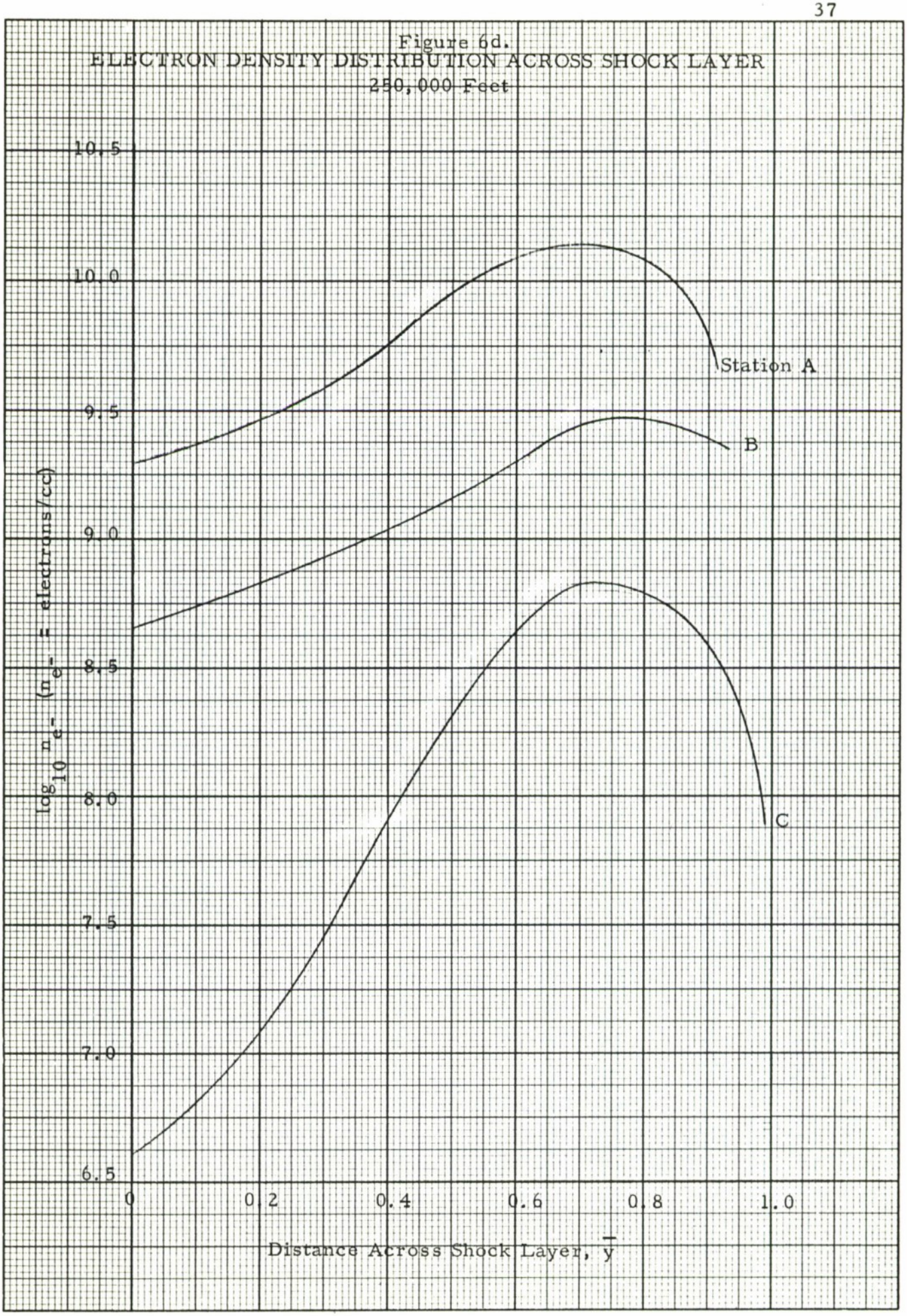

Figure 6e.

PRESSURE RATIO ACROSS SHOCK LAYER

x = 7.9
250,000 Feet

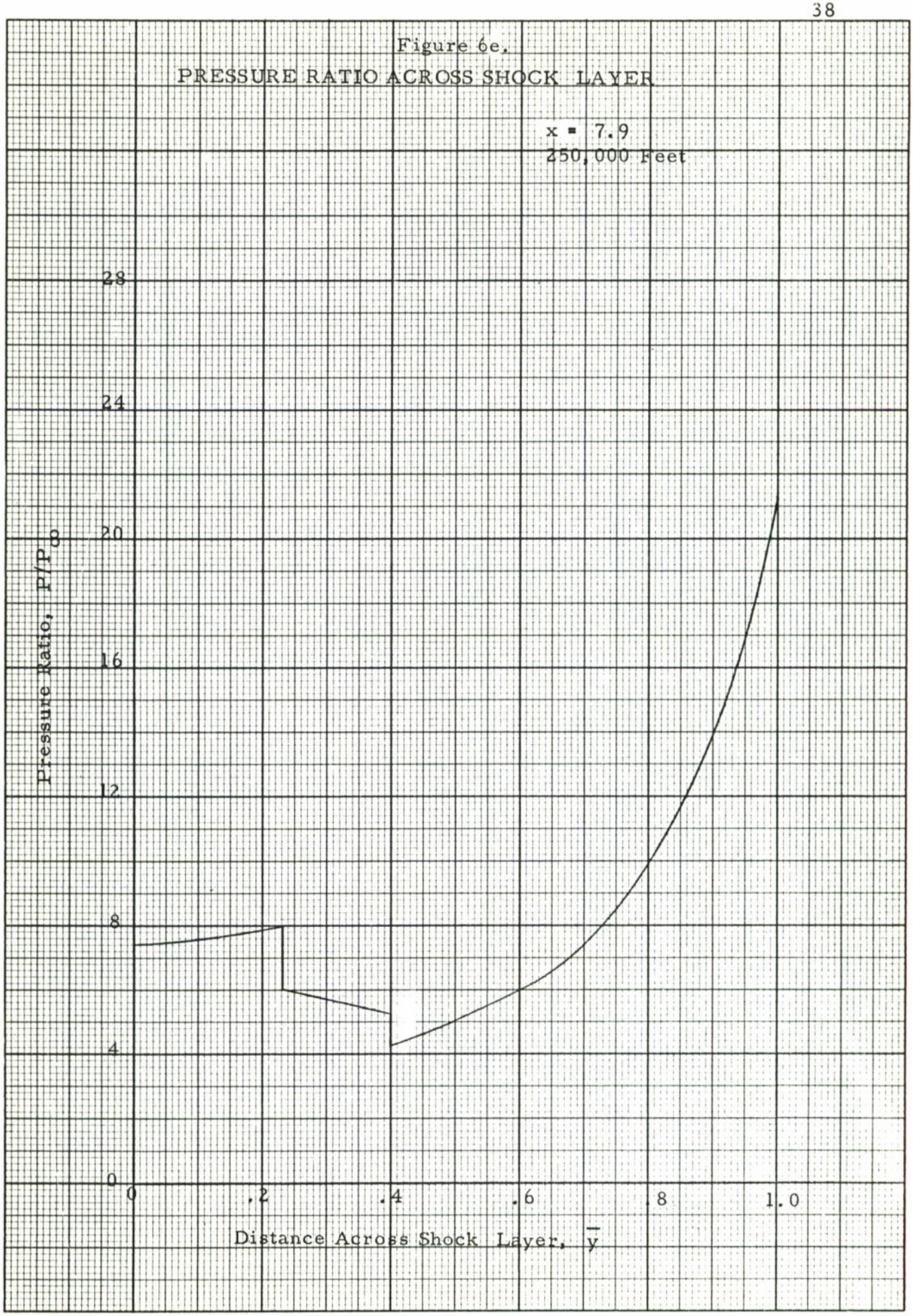

Figure 6.f.

DENSITY RATIO ACROSS SHOCK LAYER

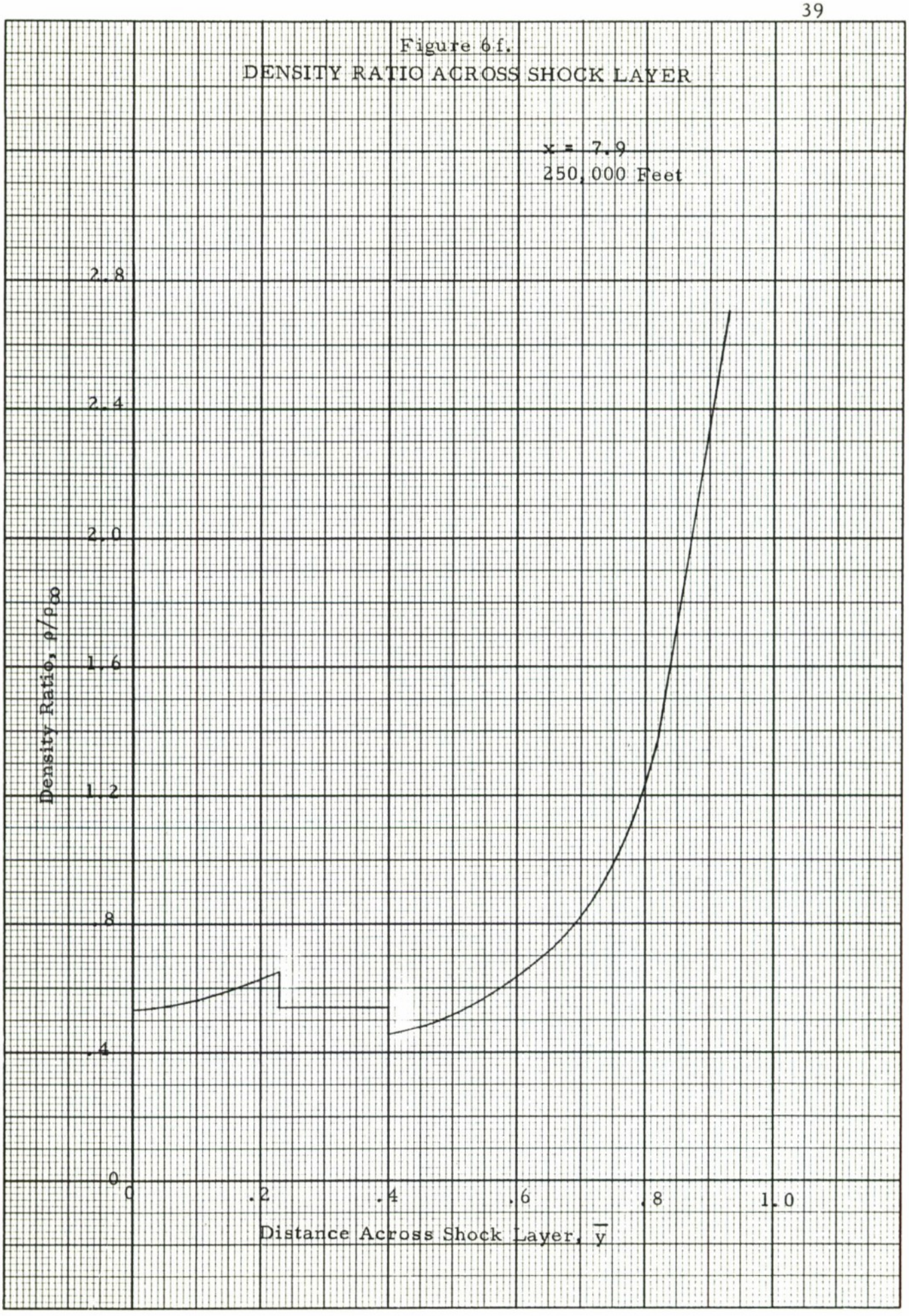

Figure 6g.

TEMPERATURE DISTRIBUTION ACROSS SHOCK LAYER

Figure 6h.

ELECTRON DENSITY DISTRIBUTION ACROSS SHOCK LAYER

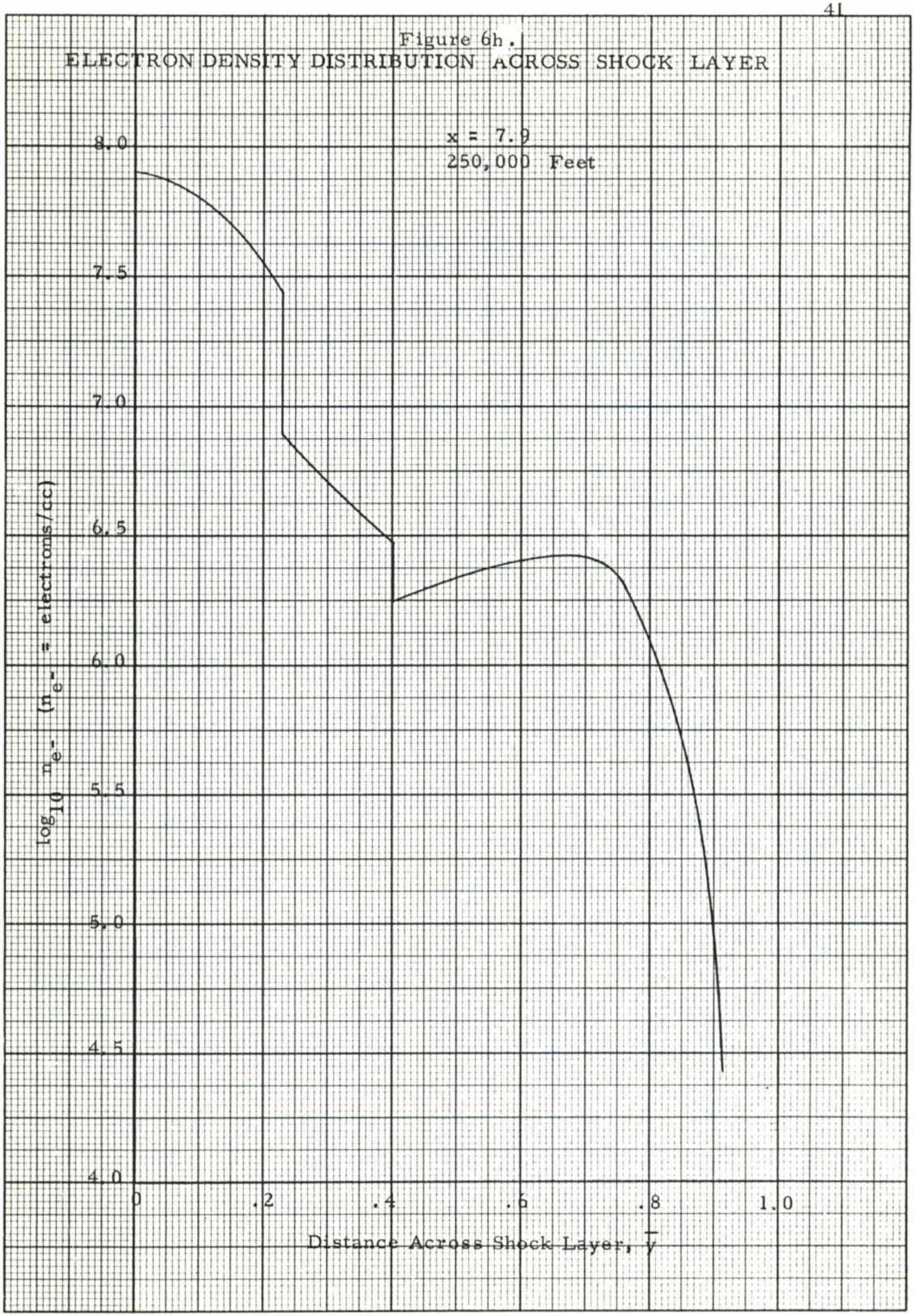

Figure 6 i.

Pressure Ratio Across Shock Layer

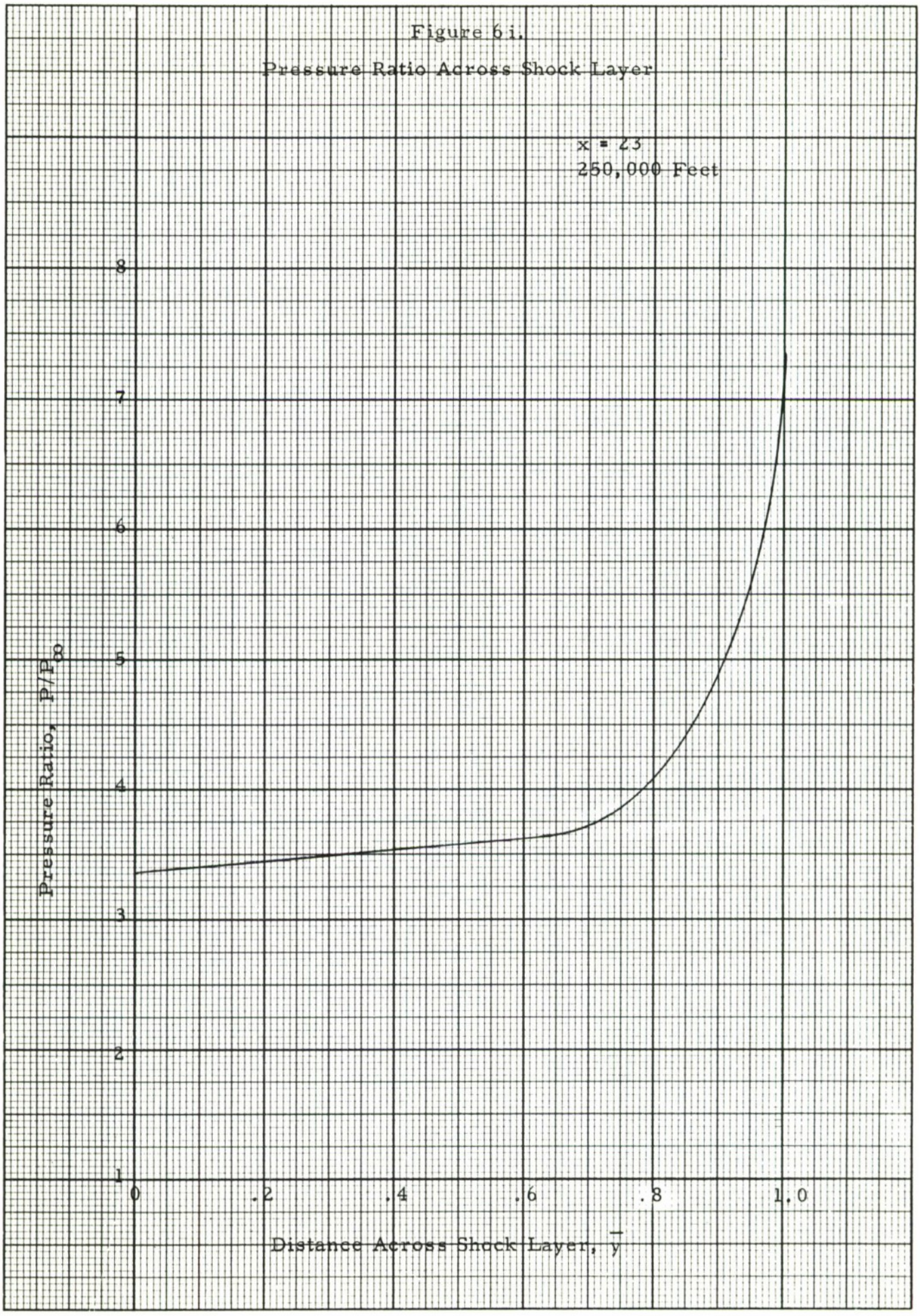

Figure 6 j.
Density Ratio Across Shock Layer

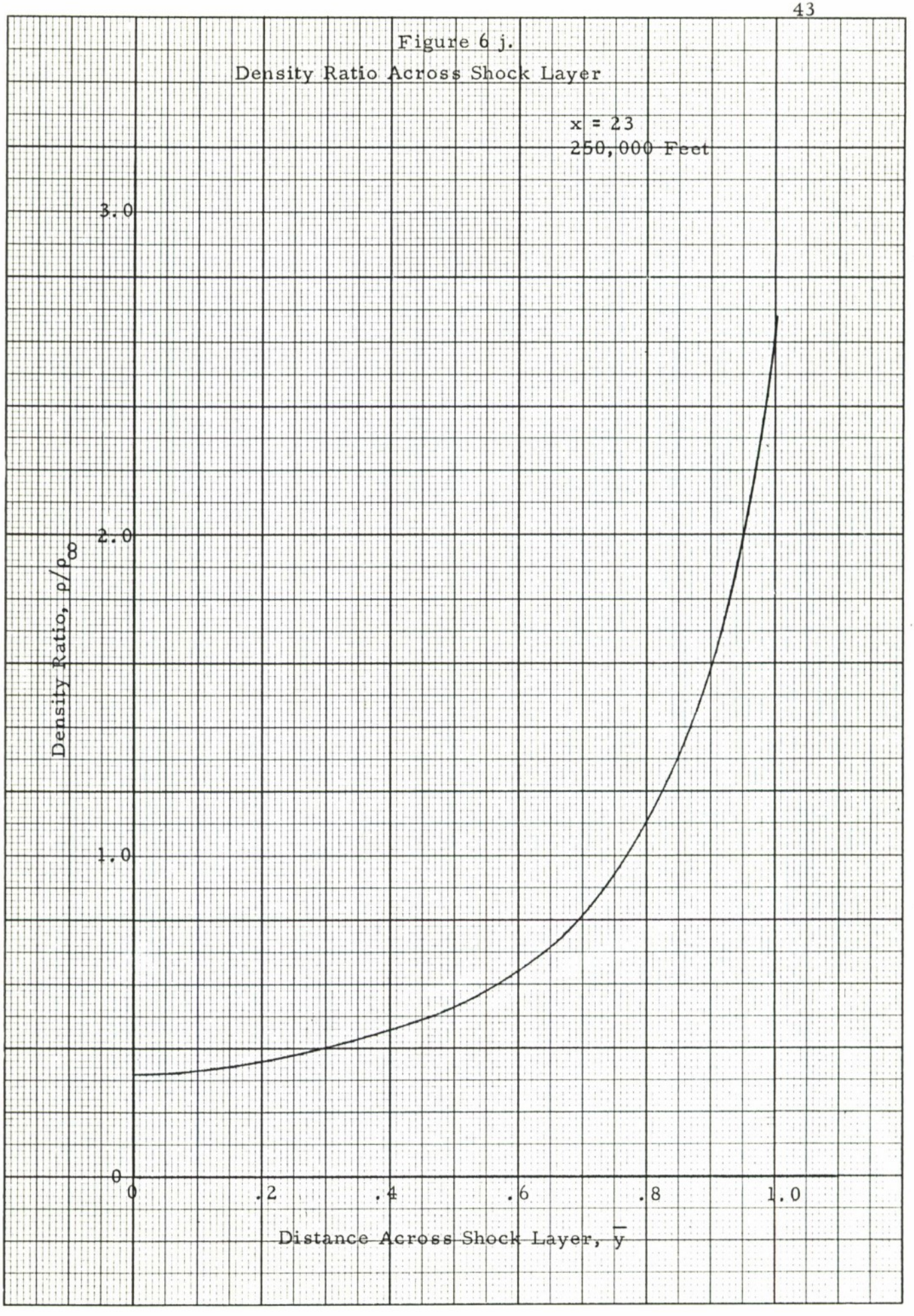

Figure 6 k.

Temperature Distribution Across Shock Layer

x = 23
250,000 Feet

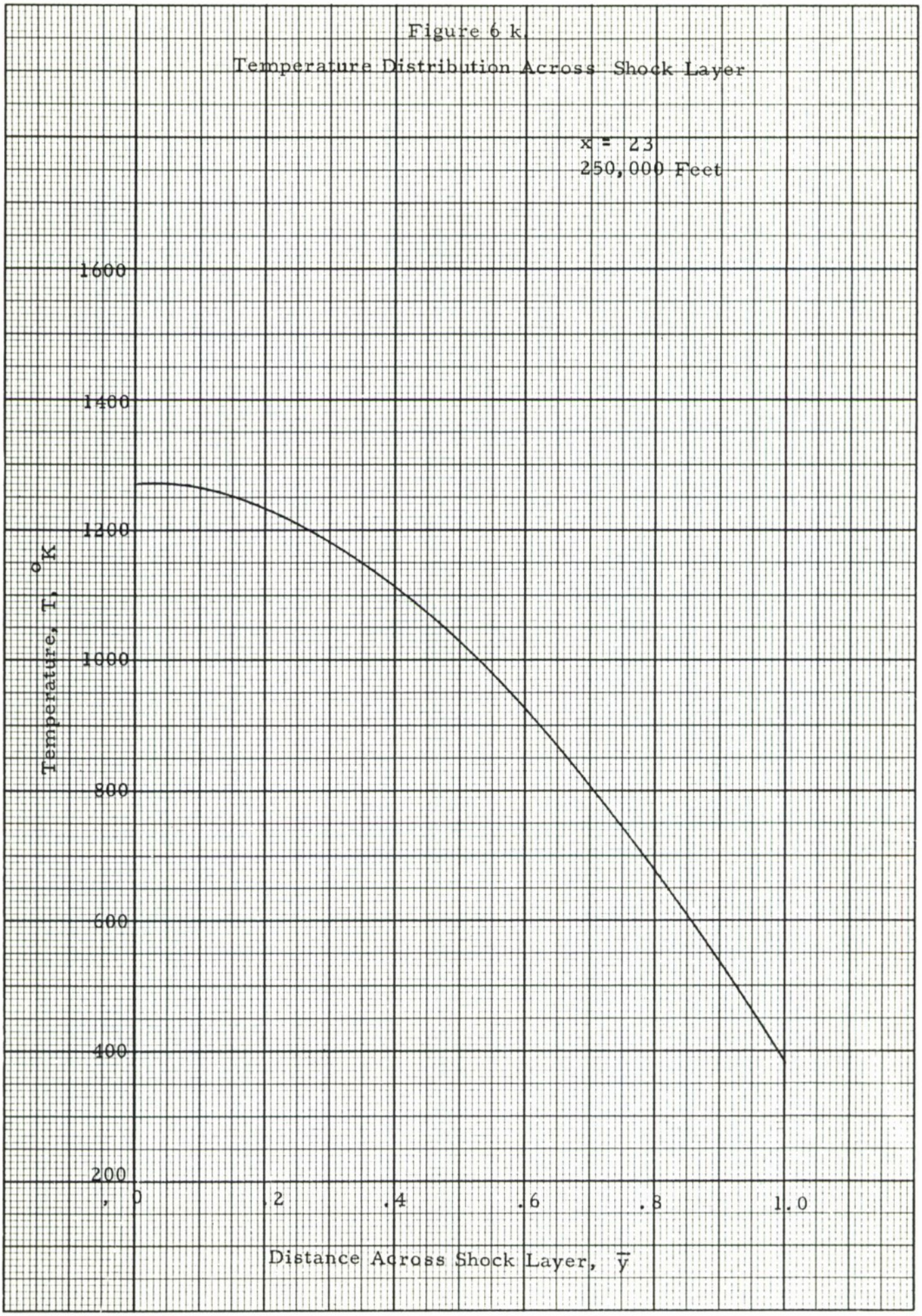

Figure 6 ℓ.

Electron Density Distribution Across Shock Layer

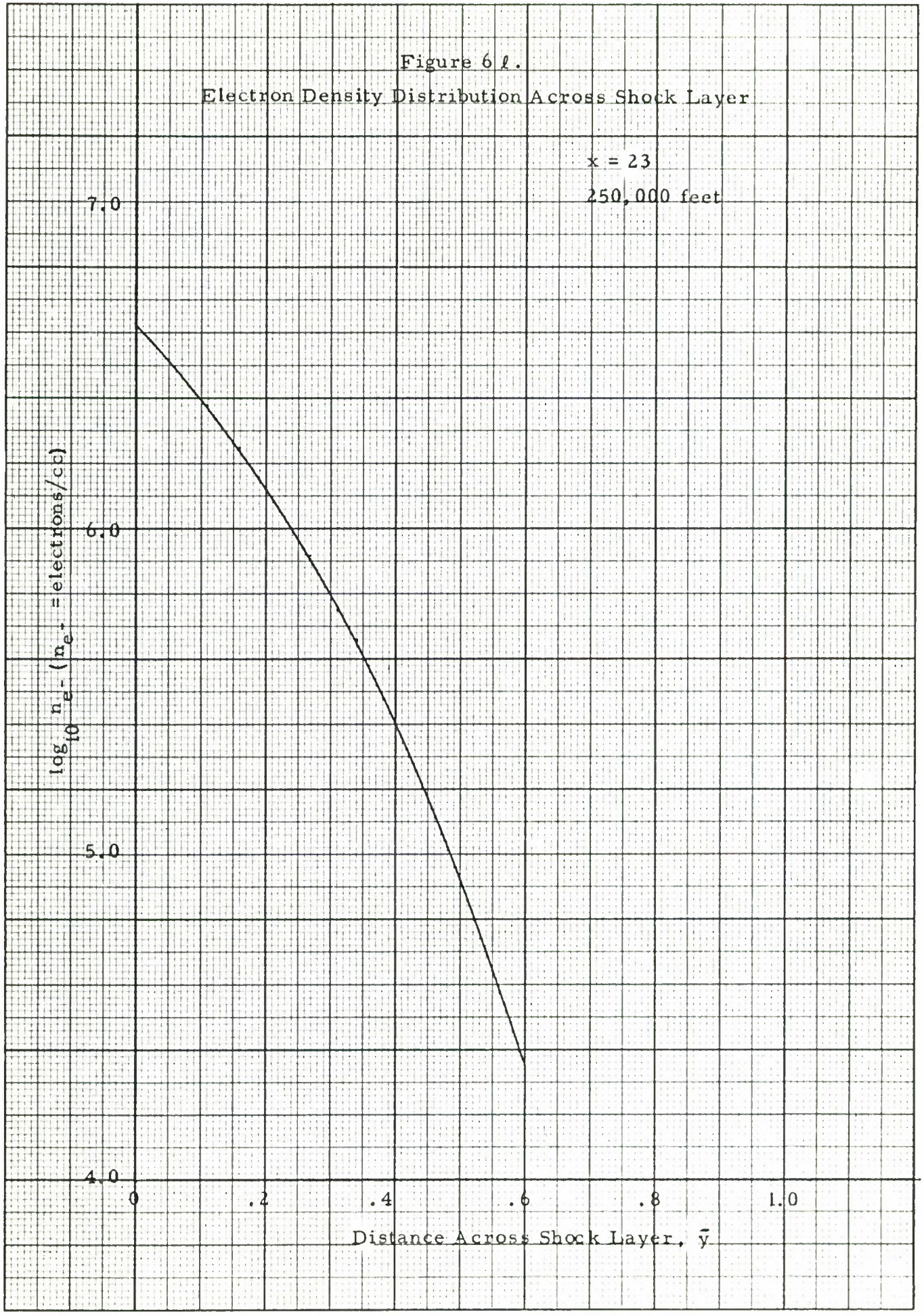

ADDENDUM TO GASL TECHNICAL REPORT NO. 231

TABLE I - MASS FRACTIONS

Streamline No.	m_{O_2}	m_O	m_N	m_{N_2}	m_{NO}
			150,000 Ft.		
1	.00014	.235	.1480	.6110	.0062
2	.00031	.233	.0963	.6627	.0093
3	.00035	.232	.0871	.6718	.0097
4	.0016	.228	.0185	.7375	.0158
5	.0088	.215	.0031	.7476	.0269
			200,000 Ft.		
1	.00005	.236	.2200	.5410	.0028
2	.00008	.236	.1941	.5669	.0033
3	.00008	.235	.1572	.6027	.0042
4	.00013	.235	.0975	.6620	.0050
5	.0146	.212	.0008	.7507	.0218
			250,000 Ft.		
1	.00001	.237	.2460	.5160	.0012
2	.00002	.237	.2190	.5427	.0015
3	.00003	.237	.1888	.5720	.0020
4	.00004	.236	.1347	.6259	.0023
5	.00064	.234	.0090	.7499	.0059

Attached: Revised Figures 1, 2 and 3.